

# CRITICAL EVALUATION OF WICKING IN PERFORMANCE FABRICS

A Thesis  
Presented to  
The Academic Facility

By  
Craig Burton Simile

In Partial Fulfillment  
Of the Requirements for the Degree  
Master of Science in the  
School of Polymer, Textile, and Fiber Engineering

Georgia Institute of Technology  
December 2004

# CRITICAL EVALUATION OF WICKING IN PERFORMANCE FABRICS

Approved by:

Dr. Haskell Beckham, Advisor

Dr. Wallace Carr

Dr. Mary Lynn Realff

November 18, 2004

## Acknowledgements

Many individuals should be thanked for the completion of this thesis. Though not all of them physically helped me, they stood by me in very trying times with numerous words of encouragement and much needed moral support. When I felt that I was unable to finish, they pushed me along and would not let me give up, for they knew failure was not an option I would be able to live with.

First and foremost, I would like to thank my thesis advisor and good “friend”, Dr. Haskell Beckham. He came to me when I was a wet-behind-the-ear undergraduate with some fabric samples. He explained to me that a company had asked him to classify these fabrics by their ability to wick moisture. Thinking this was just an easy task, I accepted the responsibility. Little did either of us know, there is no correct standard for wicking and the testing was not published in some book. No, it was much more complicated than that. Dr. Beckham explained to me that the testing would be great thesis work and I should apply to grad school to do this research. I agreed. Without his confidence that I was more than capable to trek down that path, I would not be where I am today. Dr. Beckham, even when he was on sabbatical, was always there to hear and help with my complaints, excitements, failures, and successes. He has been a real inspiration to me.

Second, I would like to thank my committee members, Dr. Wallace Carr and Dr. Mary Lynn Realff. Dr. Carr, while Dr. Beckham was on sabbatical, filled the shoes of my advisor. Being the wicking master mind of the PTFE department, he steered me in the right direction when I felt that I was lost. Without his help and skills, I may have just given up when Dr. Beckham left. Dr. Realff, little did she know, helped me as well. With the use of her skills on

the digital microscope, I was able to see my fabric samples in a different light, literally. Both these professors, even if they did not know it, were there for me when I needed them.

I can not forget Joanne Swardo at Milliken, Inc. Though I never met her and only talked to her a couple of times on the phone, my thesis could never have been completed without her. Without knowing my intentions, she sent me the fabric samples that were used in this study. While many companies turned me away, she did not.

Many people may not know of a place called Planet M, but I do. That is the name that was given to an office full of brilliant students under the leadership of Dr. Beckham. I am not sure if I am even allowed to talk about such a place, but I feel it is my duty to praise them as well. They were always there to lend a helping hand with my problems, whether the problems were technical or physiological. They always stood by me as fellow students, confidants, friends. They are some of the best people I know and I feel lucky that I was able to work next to them.

This would not be a very good acknowledgment if I did not include the great people I have had the pleasure to work with at Kimberly-Clark. Tami Mace, Thomas Oomman, Christian Sanders, Jack Lindon and Gene Verona. These are brilliant scientists that I have had the pleasure to work along side at Kimberly-Clark. They helped with many technical aspects of this thesis, as well as, just being good listeners when that is all I needed. Tami is someone though I need to put on a pedestal. She came to me with a job opportunity that may have just saved me. With funds running low and time running long, my pay at Tech was cut short. Without a job I would not make it. She knew I was capable and believed in my skills as an employee. Not only that, she is probably more critical of my work than I am. She has become, not only a great friend, but a mentor.

So many people, so little room to write about them. Of course my friends and family were always there for me and should not be overlooked. I would like to say thanks to my mom, dad, brothers, and sister. Frank and Meri, two very dear friends of mine, are also huge parts of my success. Thank you!

## Table of Contents

Acknowledgments.....	iii
List of Tables.....	viii
List of Figures.....	ix
Symbols and Abbreviations.....	xiii
Summary.....	xiv
Chapter 1 Introduction.....	1
Chapter 2 Theory and Background.....	5
2.1 Wicking and Capillarity.....	5
2.2 Fabric Capillary Pressure and Permeability.....	8
2.3 Fiber, Yarn, and Fabric Structure.....	11
2.4 Types of Wicking Tests.....	15
2.5 Vertical Wicking.....	17
2.6 Approach Proposed by Miller to Downward Wicking.....	21
2.7 New Approach to Downward Wicking.....	27
2.8 Horizontal Wicking.....	28
2.9 Combining Downward and Horizontal Wicking.....	30
Chapter 3 Experimental Procedure.....	31
3.1 Sample Selection and Preparation.....	31
3.2 Test Apparatus.....	34
3.3 Test Setup and Procedure.....	42
Chapter 4 Results and Discussion.....	47
4.1 Effects of Relative Humidity.....	47
4.2 Wicking Comparison of Distilled Water versus Perspiration.....	50
4.3 Reproducibility of Test Results.....	51
4.4 Normalizing Data.....	54
4.5 Fluid Filling Fraction.....	56
4.6 Constant Flow Rate During Downward Wicking.....	57
4.7 Vertical Wicking Results.....	58
4.8 Results for Downward Wicking as Proposed by Miller.....	60
4.9 Horizontal-Downward Wicking Results.....	64
Chapter 5 Conclusions.....	76
Chapter 6 Recommendations.....	77

References..... 78

## List of Tables

Table 3.1.1	Fabric Characteristics.....	31
Table 4.7.1	Results of vertical wicking tests.....	59
Table 4.7.2	Solutions to LaPlace equation for vertical wicking.....	59
Table 4.8.1	Downward wicking results using approach proposed by Miller.....	60
Table 4.8.2	Solutions for permeability using ratio of flow rates.....	61
Table 4.9.1	List of fluid filling fractions at changing heights.....	68
Table 4.9.2	List of wicking coefficients and y-intercepts for fabric samples.....	71
Table 4.9.3	Capillary radii and capillary pressure data for each sample at varying heights.....	72
Table 4.9.4	Solved permeability for fabric samples using Darcy's law. The units are in $\text{cm}^2$ .....	73



## List of Figures

Figure 2.1.1	Illustration of wicking in a fabric.....	5
Figure 2.1.2	Illustration of capillary rise in different size pores.....	7
Figure 2.2.1	Illustration of capillary bundles in yarns.....	8
Figure 2.3.1	Electron scanning microscope photos of cotton surface and fiber cross section.....	13
Figure 2.3.2	SEM images of the cross section and rough, scale-like structure of wool...	13
Figure 2.3.3	Fiber length and cross section images of silk taken with a SEM.....	13
Figure 2.3.4	Photomicrographs of delustered, regular nylon 66 in cross sectional and longitudinal views.....	14
Figure 2.3.5	Fiber length and cross section photomicrographs of regular Dacron polyester.....	14
Figure 2.3.6	DuPont's polyester fiber used to construct the Coolmax® fabric.....	15
Figure 2.5.1	Wicking race at different time intervals between two samples of paper towels with known pore radii. At 1 second it can be seen that sample B is the fastest, but sample A at 3 seconds and beyond catches and passes B.....	19
Figure 2.5.2	Wicking race at different time intervals between two samples of paper towels with known pore radii. At 18 seconds it can be seen that sample B is the fastest, but sample C at 81 seconds passes B.....	19
Figure 2.5.3	Wicking race at different time intervals between a paper towel and a laboratory grade filter with known pore radii. At 2 and 18 seconds it can be seen that sample C is the fastest, but the filter sample F at 180 seconds passes C.....	20
Figure 2.6.1	Miller's setup for downward wicking. The fabric sample leaves the reservoir at an acute angle $\beta$ which allows water to rise along an initial length $L_o$ before it begins its downward descent.....	21
Figure 3.1.1	Left: float stitch construction. Right: plain stitch construction.....	32

Figure 3.1.2	Compound microscope images of the technical face of sample A. The fabric was constructed using 100% polyester yarns in a float stitch pattern. Magnification – left: 16x and right: 40x.....	32
Figure 3.1.3	Compound microscope images of the technical face of sample B. The fabric was constructed using 100% polyester yarns in a plain stitch pattern. Magnification – left: 16x and right: 40x.....	32
Figure 3.1.4	Compound microscope images of the technical face of sample C. The fabric was constructed using 100% polyester yarns in a plain stitch pattern. Magnification – left: 16x and right: 40x.....	32
Figure 3.1.5	Compound microscope images of the technical face of sample D. The fabric was constructed using 86% nylon/14% spandex yarns in a plain stitch pattern. Magnification – left: 16x and right: 40x.....	33
Figure 3.2.1	Blueprint of wicking apparatus.....	34
Figure 3.2.2	BalanceTalk XL interface for wicking method.....	36
Figure 3.2.3	Photograph of apparatus inside the environmentally controlled chamber (ECC).....	38
Figure 3.2.4	Picture of top view of wicking area.....	38
Figure 3.2.5	Photograph of side view of wicking area.....	39
Figure 3.2.6	Photograph of front of wicking apparatus.....	39
Figure 3.2.7	Picture of wicking z used to immerse fabric inside reservoir.....	40
Figure 3.2.8	Photograph of sample attached to wicking z inside reservoir. Wicking z allowed fabric to be immersed inside reservoir without touching it.....	40
Figure 3.2.9	Photograph of separatory funnel which allows water to be delivered to reservoir located in side ECC.....	41
Figure 3.2.10	Picture of tubing into reservoir from separatory funnel.....	41
Figure 3.3.1	Vertical wicking setup.....	42
Figure 3.3.2	Plot of flow rate versus $L_o$ using sample D at a vertical rise of 1.5 cm. The linearity of the line proves that the choice of $L_o$ is arbitrary in solving Darcy's law.....	45
Figure 3.3.3	Arrangement for carrying out horizontal-downward wicking method.....	45

Figure 4.1.1	Effect of relative humidity on a beaker of water at a temperature of 22 °C.....	48
Figure 4.1.2	The effects of relative humidity on the results obtained using sample D when conducting a downward wicking test. The temperature was maintained at 22 °C.....	49
Figure 4.2.1	Downward wicking comparison using distilled water, tap water, and sweat simulant as wicking fluid.....	51
Figure 4.3.1	Three repetitions of a horizontal-downward wicking test using sample A. The test was conducted at a height of 1.5 cm and a horizontal length of 20 cm.....	52
Figure 4.3.2	Three repetitions of a horizontal-downward wicking test using sample B. The test was conducted at a height of 1.5 cm and a horizontal length of 20 cm.....	53
Figure 4.3.3	Three repetitions of a horizontal-downward wicking test using sample C. The test was conducted at a height of 1.5 cm and a horizontal length of 12 cm.....	53
Figure 4.4.1	Comparison of various ways to analyze wicking data. Visual (◇) refers to data recorded by watching moisture front as it traveled along fabric sample. Normalized (○) refers to mass data obtained by balance and computer program that were normalized using Equation 4.4.1. Using fluid filling fraction (Δ) refers to the method for solving length using Equation 2.6.21.....	55
Figure 4.5.1	Fluid filling fractions in 2-centimeter increments of sample D. The height of the test was 1.5 cm.....	56
Figure 4.6.1	Plot of length versus time for a horizontal-downward wicking test using sample D. Data was obtained by visual inspection of the moisture. Dot indicates the start of downward wicking.....	57
Figure 4.6.2	Plot of flow rate versus length for a horizontal-downward wicking test using sample D. Dot indicates start of downward wicking.....	58
Figure 4.8.1	Plot of $dL/dt$ versus $1/L_0$ for sample D using Miller's downward wicking method.....	62
Figure 4.8.2	Downward wicking results for Coolmax polyester using Miller's method.....	63
Figure 4.9.1	Horizontal-downward wicking test results for sample A.....	64

Figure 4.9.2	Horizontal-downward wicking test results for sample B.....	65
Figure 4.9.3	Horizontal-downward wicking test results for sample C.....	65
Figure 4.9.4	Downward data for sample A. Associated flow rates are labeled at the top of each set of data for a given test. $L_o = 20$ cm.....	66
Figure 4.9.5	Downward data for sample B. Associated flow rates are labeled at the top of each set of data for a given test. $L_o = 20$ cm.....	67
Figure 4.9.6	Downward data for sample C. Associated flow rates are labeled at the top of each set of data for a given test. $L_o = 12$ cm.....	67
Figure 4.9.7	Horizontal segment of test method for sample A following the Lucas-Washburn equation.....	69
Figure 4.9.8	Horizontal segment of test method for sample B following the Lucas-Washburn equation.....	70
Figure 4.9.9	Horizontal segment of test method for sample C following the Lucas-Washburn equation.....	70
Figure 4.9.10	Plot of permeability as a function of fluid filling fraction. Sample B has the highest permeability at higher saturation, but drops below that of sample A after a fluid filling fraction of 0.55.....	74

### Symbols and Abbreviations

Symbol or Abbreviation	Meaning	units
$A$	Flow area perpendicular to length	$\text{cm}^2$
$dL/dt$	Flow rate	$\text{cm/s}$
$dV/dt$	Volumetric flow rate	$\text{cm}^3/\text{s}$
$dM/dt$	Mass flow rate	$\text{g/s}$
$f$	Fluid filling fraction	-
$F$	Miller's ratio	-
$g$	Gravitational constant	$\text{cm/s}^2$
$h$	Hydraulic head	$\text{cm}$
$K$	Hydraulic conductivity	$\text{cm/s}$
$k$	Permeability	darcy or $\text{cm}^2$
$L$	Downward flow length	$\text{cm}$
$L_c$	Height of liquid column that would produce equivalent $P_c$	$\text{cm}$
$L_o$	Initial flow length or horizontal flow length	$\text{cm}$
$P_c$	Capillary Pressure	$\text{dyne/cm}^2$
$P_h$	Hydrostatic Pressure	$\text{dyne/cm}^2$
$R$	Effective capillary radius	$\text{cm}$
$t$	time	$\text{s}$
$W_c$	Wicking coefficient or rate constant	$\text{cm/s}^{1/2}$
$\gamma$	Liquid surface tension	$\text{dyne/cm}$
$\eta$	Fluid viscosity	centipose or $\text{dyne s/cm}^2$
$\theta$	Contact angle	-
$\rho$	Liquid density	$\text{g/cm}^3$

### Constants Used for Water

Symbol	Meaning	Value
$\gamma$	Surface tension	72.8 $\text{dyne/cm}$
$\eta$	Viscosity	0.01 $\text{dyne s/cm}^2$
$g$	Gravitational constant	980 $\text{cm/s}^2$
$\rho$	density	1.0 $\text{g/cm}^3$

## Summary

A method used to calculate the fundamental properties that predict the overall wicking performance of a fabric was proposed and executed. The combination of a horizontal and downward wicking test provided detailed measurements of the pertinent properties to wicking performance: capillary pressure and permeability. This method was proposed due to flaws found in standard vertical wicking tests as well as erroneous assumptions made in other wicking tests. Assumptions that capillary pressure and permeability are characteristic constants of porous structures are incorrect and will produce misleading information about that substrate. It was experimentally proven that these properties were a function of the saturation level found within the voids of a fabric. To obtain relevant capillary pressure and permeability data for a given fabric, a range of saturation levels were tested and analyzed. It was shown that saturation levels decreased as the vertical distance traveled by moisture increased. This phenomenon occurs as a result of capillary pressure within the voids dropping below the functional range needed to support flow in those voids at increasing heights. As height is increased, capillary pressure needs to also increase; therefore, only smaller radii pores will fill. Once saturation levels are known at specific heights, capillary pressure and permeability calculations were made using Darcy's law and the Lucas-Washburn equation. Although this phenomenon is well known in civil engineering, it has not been widely addressed in the textile sciences, especially in its implications for wicking tests.

## **Chapter 1**

### **Introduction**

Synthetic polymer fibers are playing a significant role in industry for special end use applications. One of the applications involves the formation of yarns to be made into performance fabrics through knitting or weaving. Performance fabrics, for purposes of this paper, are defined as fabrics used in specialty apparel and gear that are engineered for use in high-energy sports and activities performed in extreme environments. Clothing made of performance fabrics are said to be designed not only for fashion or just a passive cover for the skin, but to critically influence the comfort and performance of the wearer. Mills and manufacturers have engineered these fabrics to manage moisture, regulate temperature, and provide protection from the surrounding environment. They are designed to interact with and modify the heat-regulating function of the skin as the surrounding environment interacts with them<sup>1</sup>.

Mainly, performance fabrics are engineered to keep the body dry during vigorous athletic activities. Keeping the body dry, especially during cold weather sports, ensures that the wearer does not lose heat unnecessarily by having wet skin. Interaction of a fabric with moisture affects the two main categories of body comfort: sensorial and thermophysiological (thermal)<sup>2</sup>. Sensorial comfort pertains to the satisfaction of the wearer as the fabric or garment is perceived by the basic senses of the body<sup>3</sup>. This type of comfort may be affected by how a fabric feels against the skin, how it appears to the eye, how it smells, or even how it sounds. In the case of performance fabrics worn in hot climates, how a fabric feels to the wearer is one of the most important attributes. Performance fabrics help to ensure that the athlete does not start to feel clammy because, in general, “dry feels better.” Thermophysiological comfort describes how the

fabric controls the microclimate, which is the air encompassing the body. This type of comfort is crucial during activities performed in colder climates. For example, polyester based fabrics do not conduct heat, therefore, the air between the body and the fabric increases in temperature due to entrapment of body heat. This is one of the reasons why polyester is used as a base layer in cold weather sports. If the base layer fabric adsorbs and retains moisture it loses this property and its ability to keep the body warm. In general, this type of comfort describes how hot or cold the fabric makes you feel.

The human body is exceptionally self regulating and sweat is produced to keep the core temperature down. During athletic activity, the human body produces heat and a certain amount of water vapor. If the heat emission is no longer sufficient to keep the core temperature of the body at about 37 °C, the body will also produce liquid sweat<sup>4</sup>. The optimum form of sweat utilization is the evaporation of moisture directly from the skin to be released as water vapor<sup>4</sup>. This is true because most of the heat energy needed to evaporate the moisture is extracted from the body causing body temperature to drop. Only via the evaporation of liquids can the body efficiently cool itself at high physical loads, which has served as a primary motivation for an increasing interest in the transport of liquids through clothing systems<sup>5</sup>. Also, the heat flow from the skin through the clothing can be considerably greater when the clothing is wet, since water decreases the thermal insulation of clothing<sup>6</sup>. This happens because water has a greater thermal conductivity than air. Matter of fact, water cools the body twenty-five times faster than air. That is why if someone were to place their hand in a bath of water at 40 °F it would feel colder than air at the same temperature.

In normal stationary conditions, the human body produces little sweat or saturated water vapor. Thus, the wearer may not experience any significant difference in comfort while wearing



clothing made of natural or synthetic fibers, which have different water vapor transmission characteristics<sup>1</sup>. It has been shown though, that the quantity of sweat produced by test subjects wearing clothing made of cotton was less than that with a polyester article<sup>4</sup>. This happens because most synthetic fibers are not adequate conductors of heat, while cellulosic fibers are excellent conductors of heat. As good conductors of heat, they carry warmth away from the body and are favored for use in hot weather<sup>7</sup>. Consequently, most natural fibers absorb moisture and dry very slowly. The moisture retained in the fabric can cause a “post exercise chill” in a rest phase if the clothing is in contact with the skin. This “post exercise chill” can be exceedingly uncomfortable and can lead to dangerous hypothermia. If one can wear clothing next to the skin that does not pick up any moisture, but rather passes it through to a layer away from the skin, heat loss at rest will be reduced<sup>6</sup>. Most synthetic fabrics have low absorbency as well as excellent wicking properties that make them more comfortable to wear, since perspiration can travel to the surface of the fabric where it evaporates<sup>7</sup>.

In order to keep the body dry, the fabric must be able to transport the moisture away from the skin either through diffusion or wicking. Wicking has become a major topic in today’s athletics, which has given birth to many new companies and products. From fibers to apparel, these companies are flooding the athletic market with products that claim to keep the athlete dry and comfortable. Companies like Under Armour, Coville, and DuPont have emerged into the athletic apparel market with products that are claimed to be revolutionary. Under Armour claims that they have “engineered the ultimate Moisture Transport System in garments that slide over your body like a second-skin to keep you cool, dry and light throughout the course of a game or workout.” Coville Inc., a knitted fabric manufacturer, states that their “process of topically treating polyester [Polygon] provides superior wicking and transport of vapor away from the

body to the garment surface where water can evaporate.” Also DuPont, a company with a broad range of products, have engineered a “fast wicking” polyester fabric called Coolmax®. Coolmax® is said to “move perspiration away from the body to the fabric's outer surface, where it can evaporate quickly.” This thermoregulatory effect helps consumers stay drier and more comfortable according to DuPont. Are these companies, and other companies like them, selling products that do exactly what they promise? An average consumer may not understand what wicking is or the characteristics of a good wicking fabric. That is because a quantitative definition of wicking is lacking and claims are easily made for fabrics that are said to be the best. This research is expected to provide an insight not only to consumers, but also industry, on fabric properties that make up a good wicking garment.

Wicking, as the transport of perspiration in liquid form, is claimed by some authors but disputed by others as an important contributor to the thermal comfort of fabrics worn next to the skin<sup>8</sup>. The attempts to quantify wicking have given rise to many test methods, which in turn have led to abundant confusion because of the diversity of the results. The data presented in this report attempts to bring insight into some of the models that have been proposed for the wicking of moisture in performance fabrics. Why has wicking become such a concern with performance fabrics? In general, the faster a fabric can wick moisture, the more surface area the moisture covers, in turn allowing the evaporation of the moisture to occur faster leaving the wearer dry and comfortable. Knowledge of flow properties is essential in the design and application of performance fabrics.

## Chapter 2

### Theory and Background

#### Section 2.1 – Capillarity and Wicking

The term wicking has taken on many definitions and has been the subject of many research papers. In general, wicking takes place when a liquid travels along the surface of the fiber but is not absorbed into the fiber. Physically, wicking is the spontaneous flow of a liquid in a porous substrate, driven by capillary forces. This type of flow in any porous medium, caused by capillary action, is governed by the properties of the liquid, liquid-medium surface interactions, and geometric configurations of the pore structure in the medium<sup>9,10</sup>. Liquid properties such as surface tension, viscosity, and density, as well as the surface wetting forces of the fibers are known or can be experimentally determined, but the pore structure of a fibrous medium is complicated and much more difficult to quantify. The complexity of a fabric structure makes it impossible to measure an accurate pore structure. Furthermore, movement and interaction of a liquid through pores can cause both shifting of fibers and changes in pore structure<sup>9,10</sup>. Changes in fiber properties caused by wetting can significantly alter liquid movement. Figure 2.1.1 below shows the movement of liquid perspiration into a fabric from the skin. The wicked moisture spreads throughout the fabric allowing the moisture to easily evaporate.

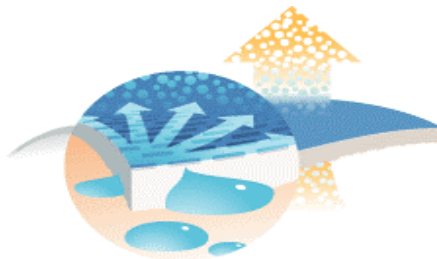


**Figure 2.1.1** – Illustration of wicking in a fabric<sup>11</sup>.

Wicking in fabrics may occur in a range of conditions and situations. Ghali<sup>12</sup> *et. al.* believes that “to define this range of conditions, researchers attempt to distinguish between two phenomena related to liquid transport in fabrics – wettability and wickability.” Qualitative definitions of these terms can be found in the literature but parameters which quantify these properties are not available. According to Harnet and Mehta<sup>8</sup>, “wickability is the ability to sustain capillary flow,” whereas wettability “describes the initial behavior of a fabric, yarn, or fiber when brought into contact with water.” While wetting and wicking are still argued to be separate phenomena, they can be described by a single process – liquid flow in response to capillary pressure<sup>12</sup>. More completely, in the absence of external forces, the transport of liquids in a porous media is driven by capillary forces that arise from the wetting of the fabric surface. Because capillary forces are caused by wetting, wicking is a result of spontaneous wetting in a capillary system<sup>13</sup>. Hence, they are coupled and one cannot occur in the absence of the other.

The spontaneous flow of moisture or wicking occurs due to a pressure differential or capillary action. Capillary action, or capillarity, can be defined as the macroscopic motion or flow of a liquid under the influence of its own surface and interfacial forces. The primary driving forces responsible for the movement of moisture along the fabric are the forces of capillarity. Capillarity describes the phenomenon when liquids in narrow tubes, cracks, and voids take on motion caused by the surface tension of the liquid. Capillarity is based on the intermolecular forces of cohesion and adhesion. If the forces of adhesion between the liquid and the tube wall are greater than the forces of cohesion between the molecules of the liquid, then capillary motion occurs. This flow is similar to other types of hydraulic flow in that it is caused by a pressure difference between two hydraulically connected regions of the liquid mass<sup>14</sup>. The direction of flow is such as to decrease the pressure difference. Flow would cease when the

pressure difference became zero. According to the laws of capillarity, fluid flow would be faster in a void with a large capillary radius than that in one with a small radius. Though that may be true, the smaller radius capillary can transport moisture to a greater height as illustrated in Figure 2.1.2 below.

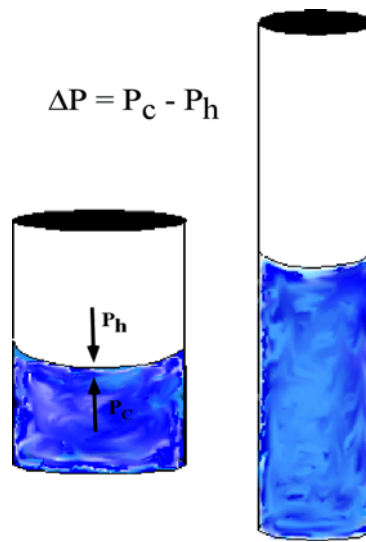


**Figure 2.1.2** – Illustration of capillary rise in different size pores

Unlike a capillary of a given dimension, the capillaries that constitute the flow boundary in a yarn are made up of a distribution of pore radii. Due to the mechanisms of capillarity, the moisture front moves from the larger pores to the smaller pores as height increases. This would indicate that the moisture flows from a region of low capillary pressure to a region of high capillary pressure. In general, the moisture begins in all the pores, but can travel only to certain heights in the larger pores where it then migrates to the smaller pores. So as the height increases, moisture held in the yarns of a fabric decreases because all pores are not filling. If the pores or capillaries do not fill, then they do not contribute in the transport or wicking of the moisture. The terms capillary, pore, and void are used interchangeably throughout this thesis.

## Section 2.2 – Fabric Capillary Pressure and Permeability

The two fundamental properties used to predict overall wicking performance in a fabric is capillary pressure and permeability<sup>15</sup>. As explained in the previous section, capillary pressure is the primary driving force responsible for the movement of moisture along a fabric. The magnitude of capillary pressure  $P_c$  can be expressed by the LaPlace equation:

$$P_c = \frac{2\gamma \cos \theta}{R} \quad (2.2.1)$$

where  $\gamma$  is the liquid surface tension,  $\theta$  is the contact angle of the liquid with the substrate, and  $R$  is the effective capillary radius. As stated earlier, a textile fabric is commonly classified as a medium made up of many capillaries; therefore, it must follow the same rules of capillarity described in Section 2.1. Numerous assumptions are made, though, when characterizing the capillary structure of the fabric. Most importantly the capillaries formed from the fibers in the yarns are assumed to be cylindrical in shape. It is known that the channels formed by the interyarn and intrayarn spaces are not cylindrical and most frequently they are not even closed at either the sides or the ends<sup>16</sup>. They might, however, be considered analogous to a network of tubes. Imagine a fabric to be a bundle of capillaries, as illustrated in Figure 2.2.1; the capillary pressure of such a medium would be dependent on the amount of fluid held within the bundles. Unlike the single capillary, a constant capillary pressure is not relevant for bundles consisting of a distribution of pore radii as a function of height.

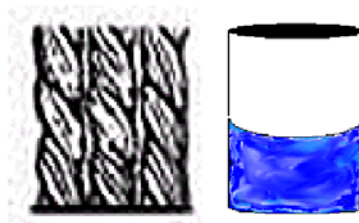


**Figure 2.2.1** – Illustration of capillary bundles in yarns<sup>17</sup>.

The other fundamental property, permeability, is the term used for the conductivity of the porous medium with respect to permeation by a Newtonian fluid<sup>18</sup>. In general, permeability is a quantitative measure of the ability of a porous medium to conduct fluid flow and is considered the one of most important physical properties of that porous medium. Permeability is related to the pore sizes and their distribution since the distribution of the sizes of entrances, exits, and lengths of the pore walls make up the major resistances to flow. Greenkorn<sup>19</sup> states that “the permeability is the single parameter that reflects the conductance of a given pore structure.” Though there are several methods to solve for the permeability in porous media, they usually involve a nonwetting liquid or air be forced through the substrate. This through-plane permeability does not accurately define the property of the medium to wick moisture. To assess wicking, one must be able to calculate an in-plane, nonforced permeability. This type of permeability quantitatively helps to define how a fabric can wick moisture. Solving for this type of permeability using Darcy’s law will be introduced in Section 2.5

The units of permeability are given in terms of darcies. One darcy is the permeability of a solid through which one cubic centimeter of fluid, having a viscosity of one centipoise, will flow in one second through a section one centimeter thick and one square centimeter in cross section. This remains true only if the pressure difference between the two sides of the solid is one atmosphere. It turns out that permeability has the same units as area; since there is no SI unit of permeability, square meters are used. One darcy is equal to about  $0.98692 \times 10^{-12}$  square meter.

Since permeability and capillary pressure are dependent on the fluid content that is held within the pores, one can not quantify the two variables without having some knowledge of the saturation level within the medium. The term “saturation” is commonly used to define the liquid

content of a porous medium. With respect to a fabric, saturation is defined as the fraction of the void spaces that is filled with a liquid. At zero saturation, there is no liquid present in the fabric, while at 100% saturation all void spaces in the fabric are filled. Governed by the laws of capillarity, saturation decreases as column height increases due to the pressure gradient on the larger capillaries to be zero, causing the movement of moisture to cease. Capillary pressure, on the other hand, increases with increasing height. This will be shown to be due to the fact that the effective capillary radius  $R$  is smaller at lower saturation. Permeability also varies greatly with saturation and reaches zero at low saturation but increases as the pores fill with water<sup>12</sup>.

In order to correctly solve for the permeability and capillary pressure in a fabric one must first be able to quantify the level of saturation in the sample. By definition, a fabric can theoretically be at 100% saturation; however, this does not accurately depict how much of the moisture actually fills the voids within the intrayarn spaces. This is because not all liquid in a completely saturated fabric is necessarily involved in capillary flow, and the definition of saturation does not differentiate between “capillary liquid” and “noncapillary” liquid<sup>12</sup>. Therefore, a measure of saturation needs to be introduced. When obtaining the level of saturation in a fabric, it is the fluid filling fraction which more accurately defines the level of moisture in the medium. Fluid filling fraction can be determined by the use of the equation:

$$f = \frac{V_{fluid}}{V_{total}} \quad (2.2.2)$$

where  $V_{fluid}$  is the volume of the liquid present in the fabric and  $V_{total}$  is the total volume of the fabric through which the fluid travels. The volume that is occupied by the liquid can be calculated by:

$$V_{fluid} = \frac{(M_w - M_d)}{\rho} \quad (2.2.3)$$



where  $M_w$  is the mass of wetted fabric section,  $M_d$  is the mass of dry section, and  $\rho$  is the fluid density (water = 1 g/cm<sup>3</sup>).  $V_{total}$  can be calculated from a knowledge of the length, width, and thickness of the fabric specimen. The calculated value of  $f$  is a measure of saturation and can be used to quantify the wicking characteristics of the tested fabrics.

### Section 2.3 - Fiber, Yarn, and Fabric Structure

A knitted textile fabric is constructed with a single yarn or set of yarns moving in only one direction. Instead of two sets of yarns crossing each other as in weaving, the single knitting yarn is looped through itself to make a chain of stitches. Because of its construction, a knitted fabric is not a completely solid structure, but is complex and porous in shape. The complex contours formed by the fibers in the yarn and the yarns in the fabric constitute the boundaries of the channels along which moisture flows<sup>16</sup>. It has been reported that the most important mechanism of fabric wicking is the motion of liquid in the void spaces between the fibers in a yarn (inrayarn)<sup>10</sup>. Due to the laws of capillarity, the much larger pores between yarns do not contribute much to the long-range motion of liquid. It has also been concluded by Minor *et al.* that yarn intersections act as new reservoirs, and feeds all branches equally<sup>16</sup>. This finding will become increasingly important when different types of knit structures are compared.

It has been theorized by many researchers that the flow of a fluid in a fabric is largely governed by the network structure of the fabric<sup>9,14,16,20,21</sup> and not due to the fiber type<sup>6,21</sup>. In any system where capillarity causes relative motion between a solid and a liquid, the shape of the solid surfaces is an important factor, which governs the rate and direction of liquid flow<sup>16</sup>. The rate of travel of liquid water is governed by the fiber arrangement in yarns which control capillary size and continuity<sup>21</sup>. To assume that fiber type does not contribute to capillary flow is

not an entirely true statement, because fiber type also contributes to the overall structure. Fiber type, under certain circumstances, can drastically change the structure of the yarn, in turn changing the wicking properties of the fabric. For example, changes in fiber properties when wet can significantly affect liquid movement and retention behaviors through fiber swelling. Fiber swelling not only increases liquid retention in the fibers at the expense of the capillary liquid capacity in interfiber pores, but also complicates the pore structure<sup>9</sup>. This swelling of the fibers can cause bottlenecking or the closing off of capillaries, which in turn causes the flow in those capillaries to be slow or even stop. It is well known that this type of response to moisture is prevalent in yarns made of cellulosic fibers<sup>7</sup>.

Also, yarns spun with natural fibers have very irregular capillaries due to various factors such as fiber roughness, cross-sectional shape and length. In yarns with fibers arranged in a relatively disorderly manner, capillary continuity is poor, and this causes changes in the water transport rate over the length of the yarn<sup>22</sup>. For example, wool fibers form rough yarns of high apparent contact angle because of the natural crimp and more random distribution of fibers in the yarns. Yarns of synthetic fibers, on the other hand, are compact, well aligned and smooth, resulting in a low contact angle<sup>22</sup>. Figures 2.3.1 through 2.3.5 below illustrate the irregular cross-section and rough surface of natural fibers versus the regular and smooth surface of synthetic fibers. The pictures were taken out of the book *Understanding Textiles*<sup>7</sup>.



**Figure 2.3.1** – Electron scanning microscope photos of cotton surface and fiber cross section<sup>7</sup>.

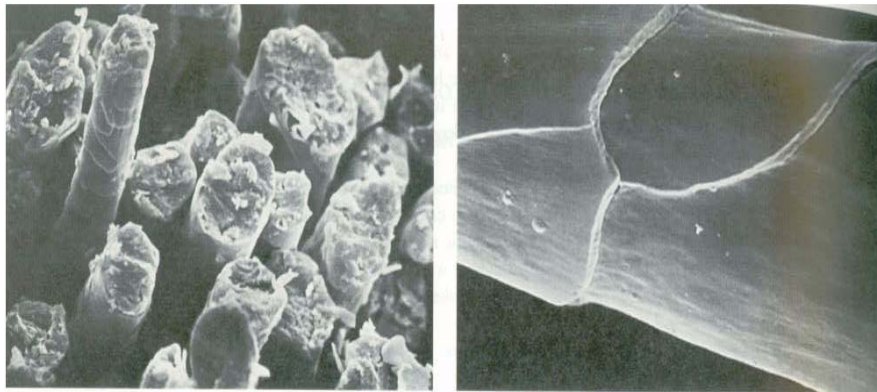


**Figure 2.3.2** – SEM images of the cross section and rough, scale-like structure of wool<sup>7</sup>.

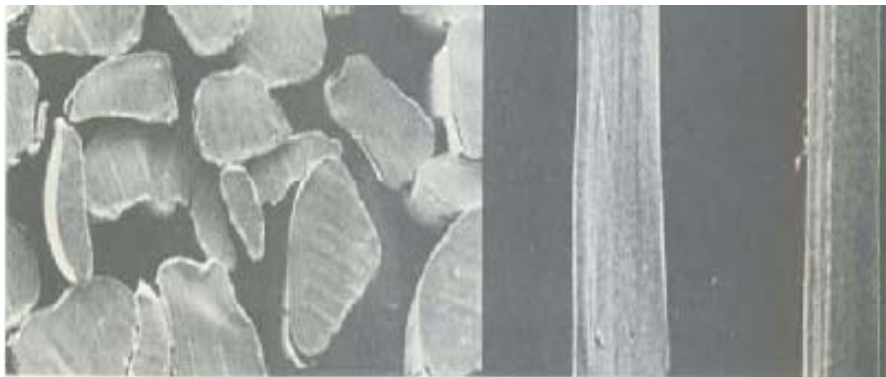


**Figure 2.3.3** – Cross section images and fiber length of silk taken with a SEM<sup>7</sup>.

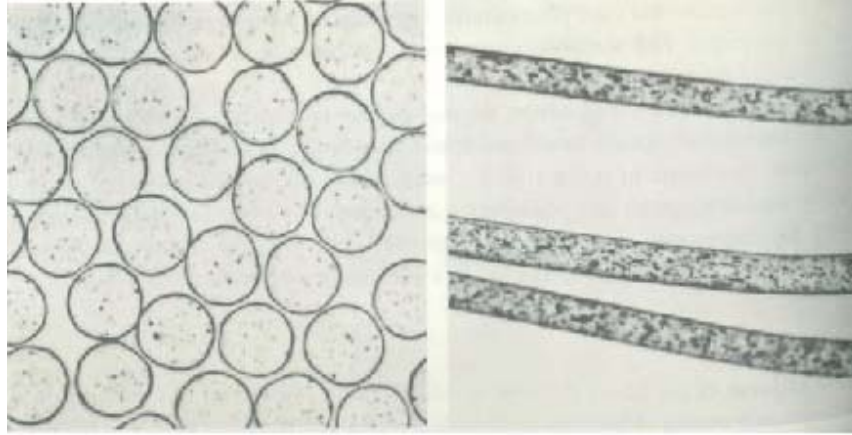


**Figure 2.3.4** – Photomicrographs of delustered, regular nylon 66 in cross sectional and longitudinal views<sup>7</sup>.

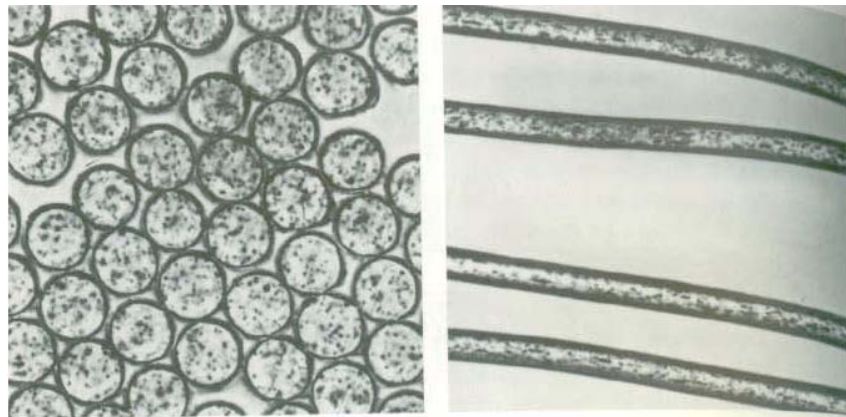


**Figure 2.3.5** – Fiber length and cross section photomicrographs of regular Dacron polyester<sup>7</sup>.

It can be easily seen why fibers derived of natural sources would not produce very regular yarns. Cotton fibers, with their flat, lima-bean-shaped cross section and ribbon like appearance, would produce very irregular capillaries within a yarn that could inhibit fluid flow. The fiber surface of wool is very rough and leads to a large fluid contact angle, which would also cause capillary flow to be hindered. Even the saying “smooth as silk” does not hold true when on a microscopic level. The fiber has a rodlike shape with occasional swelling or irregularities along its surface and a triangular cross section. Even though it is one of more regular shaped natural fibers, it would still not produce yarns as regular as those made with synthetic sources.

That can be seen by looking at the photomicrographs of polyester and nylon. They are smooth in appearance and have perfectly round cross sections with which a yarn with regular capillaries would be constructed.

Also, synthetic fibers can be manufactured to the specific needs of the fabric. The cross-section of the fiber can be altered, the lengths of the fibers can be controlled, and most importantly, yarns produced for the particular use of performance fabrics do not absorb significant amounts of moisture. Looking Figure 2.3.6, it can be seen that the polyester fiber produced by DuPont is not round, but has been modified to give, what Dupont believes, greater wicking capabilities. It will be shown that fabric construction is largely responsible for moisture flow, but fiber type must not be overlooked, especially when describing performance fabrics.

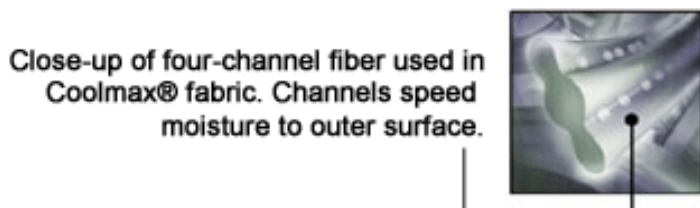


**Figure 2.3.6** - DuPont's polyester fiber used to construct the Coolmax® fabric<sup>23</sup>.

It can be generalized that the requisites for a good wicking fabric include stiff fibers, uniformity of structure, and resistance of the structure to collapse<sup>14</sup>. Also, the fibers should not be swollen by the liquid being wicked.

## **Section 2.4 - Types of Wicking Tests**

Wicking occurs when a fabric is completely or partially immersed in a liquid or in contact with a limited amount of liquid, such as a drop placed on the fabric. Therefore, capillary penetration of a liquid can occur from an infinite (unlimited) or finite (limited) reservoir<sup>13</sup>. The

different forms of wicking from an infinite reservoir are immersion, transplanar wicking, and longitudinal wicking. A spot test is a form of wicking from a limited reservoir.

A wicking “spot” test is an example of wicking from a finite or limited reservoir, and includes placing a drop of water onto the fabric and measuring the drop absorbency time or the spreading rate of the liquid within the fabric<sup>8,13</sup>. Wicking of a limited amount of liquid onto a fabric surface is a more complicated process than wicking from an infinite reservoir. One reason is due to the fact that unlike other types of porous substrates, many fabrics are not isotropic, in which case the spreading liquid does not usually form a circle with a well-defined radius<sup>20</sup>. The capillary penetration of a drop indicates several important properties of a textile fabric, including repellency, absorbency, sorption of stain, and stain resistance<sup>13</sup>.

Wicking during immersion occurs when the fabric (or fibrous assembly in general) is completely immersed in a liquid and the liquid enters the fabric from all directions<sup>13</sup>. A liquid wicking into an immersed yarn or fabric displaces most of the air in the fibrous assembly and causes it to sink. The canvas disc-wetting test measures the sinking time of a disk submerged in a liquid. Though this type of test is no longer used, the Draves test, which uses an unboiled, naturally waxed cotton skein submerged in a surfactant solution, is routinely used to evaluate wetting agents. McLaughlin *et al.*<sup>24</sup> have stated that immersion sorption is so commonplace in textile process that its complexity is usually overlooked.

Spontaneous transplanar<sup>13</sup> or transverse wicking<sup>8,25</sup> has been deemed the term used when the transmission of a liquid is through the thickness of the fabric, that is, perpendicular to the plane of the fabric. Several techniques, but no standards, have been developed to measure transplanar liquid transport into fabrics. Plate tests, for example, measure absorbency of fabrics, especially towels. The apparatus consists of a horizontal sintered glass plate kept moist by a

water supply whose height can be adjusted so as to keep the water level at the upper surface of the plate. The specimen is placed onto the porous glass plate, and the uptake of water is measured by timing the movement of the meniscus along the long horizontal capillary tube. These tests have been used as simulation of a sweating skin surface<sup>8</sup>. The problem encountered with this test method is that a pressure is applied to enhance the flow of liquid. When a fabric is compressed its structural elements are moved closer to each other, which can potentially change its absorption characteristics<sup>25</sup>. Results have been quoted for fabrics measured at 1.96 kPa, which is unrealistically high compared to many real wear situations<sup>8</sup>. Thus, studies on fabrics used in athletic apparel should allow the movement of moisture to be caused by natural driving forces such as surface tension, viscosity, and unforced capillary pressure.

Longitudinal wicking from an infinite reservoir occurs when the fabric is partially immersed in a large volume of liquid that can wet the fabric<sup>13</sup>. If the liquid does not wet the surface it will not wick into the fibrous assembly<sup>25</sup>. Many researchers have tried to use these types of tests to investigate capillary penetration of a liquid into a fabric. Three types of longitudinal wicking tests will be considered to try to define the ability of a fabric to transport moisture. The tests include vertical (upward), horizontal, and downward wicking.

## **Section 2.5 - Vertical Wicking**

Vertical wicking is a commonly misused method to describe the ability of a fabric to wick moisture. One standard test method for this type of wicking is the BS 3424: Part 18, Method 21A, which includes cutting the test specimen (150 mm x 50 mm) and drawing an indelible line across the surface of the fabric 50 mm from one end. The sample is then hung from a glass rod that is attached horizontally to a ring stand and lowered vertically into a

reservoir. The sample comes into contact with the contents of the reservoir at a perpendicular direction. The fluid is then allowed to rise along the fabric for twenty-four hours after which the length of the fluid path is measured to the nearest millimeter with reference to the indelible marked line. This distance that the liquid travels is what is designated as the extent of wicking. The standard test method may be precise, but it does not clearly state how the collected data defines the ability of a fabric to wick moisture.

Also, the test method fails to take the effects of gravity into account. When the direction of the flow of moisture is upward, gravity has an opposing effect which results in the fluid flow to slow and eventually stop. Most testing procedures that are based on upward wicking either ignore the effects of gravity or implicitly assume that it will have a similar proportional influence on all materials<sup>15</sup>. Physically, liquid in a capillary rises due to the net positive force across the liquid solid interface and is defined by:

$$\Delta P = P_c - P_h \quad (2.5.1)$$

where  $P_c$  is the capillary pressure and  $P_h$  is the hydrostatic pressure caused by gravity. If the change in pressure equals zero or negative the flow would stop. It can be inferred from the equation that the capillary pressure  $P_c$  which drives the wicking process is opposed by a continuously increasing hydrostatic head  $P_h$ , which is proportional to the height of rise:

$$P_h = \rho gh \quad (2.5.2)$$

where  $\rho$  is the liquid density,  $g$  is the gravitational constant, and  $h$  is equal to the rise of height. When capillary pressure is greater than the weight of the liquid, the positive force drives the liquid upward<sup>9</sup>. Once the moisture has reached its equilibrium height, capillary pressure is equal to the hydrostatic head, which causes the net driving force to be equal to zero, consequently



causing the moisture front to cease<sup>9</sup>. In addition, movement is opposed by viscous drag (friction), which also increases as the length of the liquid column increases.

Using the theory of capillarity and upward wicking test, one would expect moisture to flow faster in a medium with larger pore size. However, Miller<sup>15</sup>, using a competitive wicking study, showed that this is not always the case. The study was conducted with a set of household paper towels (labeled A, B, C) and a laboratory grade filter paper (F). A digital camera was used to record the motion of the liquid. The camera recordings were made at one-second intervals. Figures 2.5.1 through 2.5.3 clearly show how an “overtaking” phenomenon occurs in such materials<sup>15</sup>.

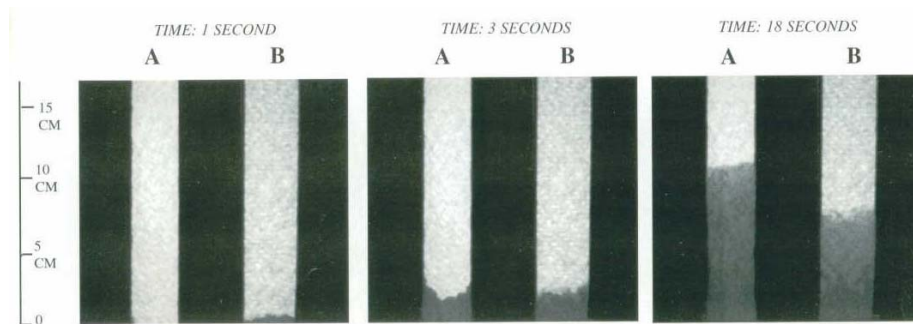


**Figure 2.5.1** – Wicking race at different time intervals between two samples of paper towels with known pore radii. At 1 second it can be seen that sample B is the fastest, but sample A at 3 seconds and beyond catches and passes B.

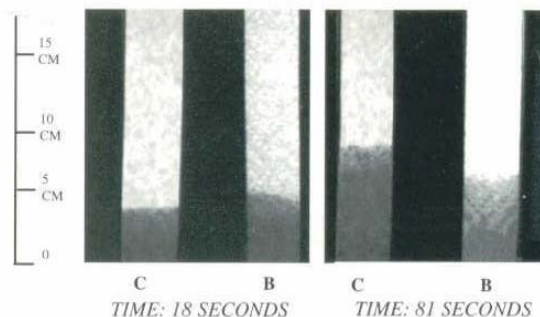


**Figure 2.5.2** – Wicking race at different time intervals between two samples of paper towels with known pore radii. At 18 seconds it can be seen that sample B is the fastest, but sample C at 81 seconds passes B.

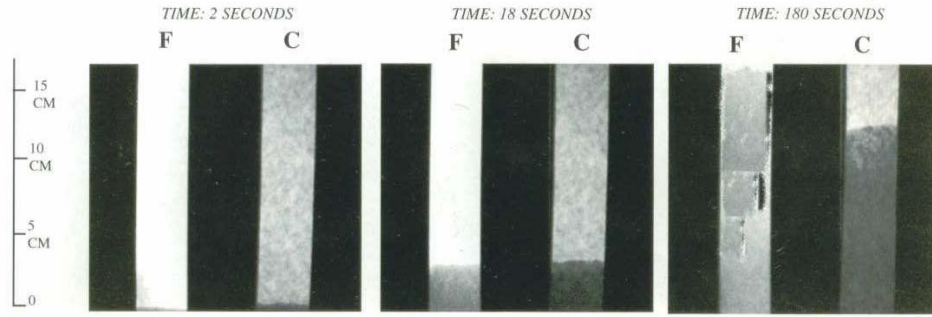


**Figure 2.5.3** – Wicking race at different time intervals between a paper towel and a laboratory grade filter with known pore radii. At 2 and 18 seconds it can be seen that sample C is the fastest, but the filter sample F at 180 seconds passes C.

This “overtaking” phenomenon, as demonstrated by the pictures, clearly shows that an upward wicking test will not be able to identify which is the fastest wicking material. Each of the four candidates used in the study was fastest at some point in time or distance. This phenomenon does not completely preclude the usefulness of an upward wicking test. The height at which the moisture front ceases can theoretically be used to calculate the capillary pressure ( $P_c$ ) of the system. Using equation 2.4.1, when  $\Delta P$  is equal to zero, capillary pressure is equal to the hydrostatic pressure and can be defined as:

$$P_c = L_c \rho g \quad (2.5.3)$$

where  $L_c$  is the height of the liquid column that would produce the equivalent of the capillary pressure (i.e. height where the moisture front ceases and the system is at equilibrium). Capillary pressure, as defined in Section 2.2, is more commonly expressed by Equation 2.2.1. Assuming the fluid makes a contact angle of zero with the fabric, one can theoretically solve for capillary radius by combining Equation 2.4.3 and the LaPlace equation. The resulting equation is:

$$R = \frac{2\gamma}{L_c \rho g} \quad (2.5.4)$$

In order for this postulation to hold true, one would have to assume that capillary pressure is a constant throughout the entire test. It has already been explained that as height increases

capillary pressure increases due to the saturation level of the fabric decreasing. It will be shown that the assumption of constant capillary pressure leads to erroneous results.

## Section 2.6 – Approach Proposed by Miller to Downward Wicking

One approach proposed by Bernard Miller of TRI Princeton<sup>15</sup> to monitor wicking and minimize the negative affects of gravity is to run downward wicking tests. His approach is based on the physics of a siphon, where the fabric is used like a tube to transport water because of a pressure gradient. Figure 2.6.1 shows the downward wicking test setup of Miller. Once the moisture front reaches the bar and begins its descent, the flow rate becomes essentially constant<sup>15</sup>. As one notices, though, downward wicking tests cannot be run without some initial upward wicking phase. The derivations and simplifications of Darcy's Law described below are those of Dr. Bernard Miller and will be applied to his approach.

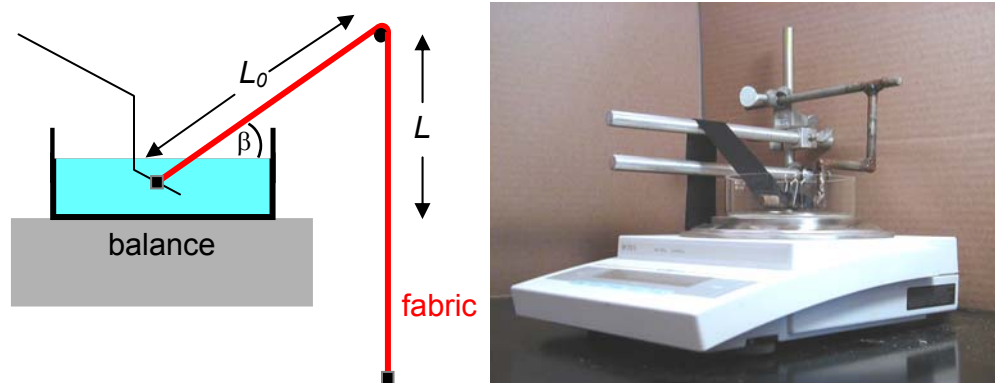


**Figure 2.6.1** – Miller's setup for downward wicking. The fabric sample leaves the reservoir at an acute angle  $\beta$  which allows water to rise along an initial length  $L_o$  before it begins its downward descent.

As stated before, a textile fabric is considered to be porous solid. Darcy's Law has been used to describe the motion of liquid through such a material. Darcy's Law was initially developed to describe water flow through sand filters, but has been used extensively in other

systems, including fibrous assemblies<sup>26</sup>. Darcy (1856) observed that the total volume of water running through sand is proportional to the loss of pressure. Darcy's law is empirical in that it is not derived from first principles; rather it is the result of experimental observation<sup>19</sup>. It is a generalized relationship for volumetric flow in porous media and can be defined as:

$$\frac{dV}{dt} = AK \left( \frac{\Delta h}{L} \right) \quad (2.6.1)$$

where  $dV/dt$  is the volumetric flow rate ( $\text{cm}^3/\text{s}$ ),  $L$  is the flow length (cm),  $A$  is equal to the flow area perpendicular to  $L$  ( $\text{cm}^2$ ),  $K$  is hydraulic conductivity ( $\text{cm/s}$ ), and  $h$  is the hydraulic head (cm). The hydraulic head at a specific point  $h$  can be written in the terms of the pressure head:

$$h = \frac{P}{\rho g} \quad (2.6.2)$$

where  $P$  is the pressure ( $\text{dyne/cm}^2$ ),  $\rho$  is liquid density ( $\text{g/cm}^3$ ), and  $g$  is the gravitational constant ( $\text{cm/s}^2$ ). The hydraulic conductivity  $K$ , defined by Darcy's law is dependent on the properties of the fluid as well as the pore structure of the medium<sup>19</sup>. Hydraulic conductivity can be written more specifically in terms of permeability and the properties of the fluids:

$$K = \frac{k \rho g}{\eta} \quad (2.6.3)$$

where  $k$  is the permeability (darcy or  $\text{cm}^2$ ) of the porous medium and in principle is only a function of the pore structure<sup>19</sup>, while  $\eta$  is the fluid viscosity expressed in centipoises or  $\text{dyne sec/cm}^2$ . With the substitution of Equation 2.6.2 and 2.6.3 into Equation 2.6.1, the volumetric flow rate can be rewritten as:

$$\frac{dV}{dt} = \frac{Ak \rho g}{L \eta} \left[ \Delta \left( \frac{P}{\rho g} \right) \right] \quad (2.6.4)$$

Simplification of Equation 2.6.4 leads to:

$$\frac{dV}{dt} = \frac{Ak}{L\eta}(\Delta P) \quad (2.6.5)$$

Volume can be calculated by multiplying length  $L$  by the cross sectional area normal to the direction of flow  $A$ . Equation 2.6.5 reduces to Equation 2.6.6 by substitution of  $V = LA$  which can be written as rate of change of length:

$$\frac{dL}{dt} = \frac{k}{L\eta}(\Delta P) \quad (2.6.6)$$

As explained by Miller, the capillary pressure ( $P_c$ ) that drives movement of the liquid against gravity is continuously opposed by an increasing hydrostatic pressure  $P_h$ , and therefore,  $\Delta P = P_c - P_h$ . The condition for upward wicking which takes into consideration the hydrostatic pressure can now be described by the velocity of a fluid with viscosity  $\eta$  moving through a porous network having a permeability  $k$ , or:

$$\frac{dL}{dt} = \frac{k}{L\eta}(P_c - P_h) \quad (2.6.7)$$

These pressure variables can be expressed in terms of liquid rise using  $P_c = L_c \rho g$  and  $P_h = L \rho g$ .

With the substitution of these terms the flow rate can be expressed as:

$$\frac{dL}{dt} = \frac{k}{L\eta}(L_c \rho g - L \rho g) \quad (2.6.8)$$

where  $L_c$  is the height of liquid column that would produce the equivalent of the capillary pressure and  $L$  is the height of rise at any time. Simplifying Equation 2.6.8 leads to the form:

$$\frac{dL}{dt} = \frac{\rho g k}{\eta} \left[ \frac{(L_c - L)}{L} \right] \quad (2.6.9)$$

As can be seen from Figure 2.6.1 for the case of downward wicking, the hydrostatic head at any time can be expressed as:

$$P_h = \rho g (L_o \sin \beta - L) \quad (2.6.10)$$

Substitution of Equation 2.6.10 into Equation 2.6.7, and knowing that the total flow length is now  $L_o + L$ , the flow rate for downward wicking becomes:

$$\frac{dL}{dt} = \frac{\rho g k}{\eta} \left[ \frac{(L_c - L_o \sin \beta + L)}{L_o + L} \right] \quad (2.6.11)$$

However, downward wicking could not take place without some initial upward wicking; after an initial deceleration, the rate of wicking becomes essentially constant. The time is recorded after the liquid moves over the bar and downward wicking begins. Since the downward wicking flow rate is at a steady state, the length  $L$  becomes arbitrary and Equation 2.6.11 can be simplified by substituting  $L_o$  for  $L$ . The general expression for the downward wicking flow rate when  $L = L_o$  becomes:

$$\frac{dL}{dt} = \frac{\rho g k}{2\eta} \left[ \frac{L_c}{L_o} + 1 - \sin \beta \right] \quad (2.6.12)$$

If two experiments are run using the same specimen, changing only the  $L_o$  distance, different constant flow rates are obtained for each run. The ratio,  $F$ , of these two rates can be used to solve for  $L_c$  in the following relationship:

$$F = \frac{\left[ \frac{dL}{dt} \right]_1}{\left[ \frac{dL}{dt} \right]_2} = \frac{\left( \frac{L_c}{L_{o1}} + 1 - \sin \beta \right)}{\left( \frac{L_c}{L_{o2}} + 1 - \sin \beta \right)} \quad (2.6.13)$$

$$F \left( \frac{L_c}{L_{o2}} \right) - \frac{L_c}{L_{o1}} = (F - 1)(\sin \beta - 1) \quad (2.6.14)$$

$$L_c = \frac{(F - 1)(\sin \beta - 1)}{FL_{o1} - L_{o2}} L_{o2} L_{o1} \quad (2.6.15)$$

Once  $L_c$  is determined, it can be substituted into Equation 2.6.12 and used with either flow rate to obtain permeability by:

$$k = \frac{2\eta L_o}{\rho g} \left( \frac{1}{L_c - L_o \sin \beta + L_o} \right) \frac{dL}{dt} \quad (2.6.16)$$

An alternative and more rigorous approach for solving Darcy's Law based on Miller's test method should be investigated due to the arbitrary nature of choosing  $L_o$  values. The general expression for downward wicking, as seen by Equation 2.6.12, can be rewritten in the form of a linear equation,  $y = mx + b$ :

$$\frac{dL}{dt} = \frac{1}{L_o} \left[ \frac{\rho g k L_c}{2\eta} \right] + \left( \frac{\rho g k}{2\eta} \right) (1 - \sin \beta) \quad (2.6.17)$$

where  $\frac{dL}{dt}$  is the dependent variable,  $\frac{1}{L_o}$  is the independent variable, the  $(\rho g k L_c)/(2\eta)$  is the slope, and the y-intercept is  $(\rho g k/2\eta)(1 - \sin \beta)$ . Using Darcy's law in this form to solve for the desired variables requires plotting a graph of  $\frac{dL}{dt}$  versus  $\frac{1}{L_o}$  and finding the equation of the line that best fits these points. To do this one must run at least two test using the same fabric sample changing only the  $L_o$ . From a linear regression analysis of the data obtained,  $k$  can be estimated from the y-intercept. Once  $k$  is estimated,  $L_c$  can be found using the slope of the line.  $L_c$  can then be used to solve for capillary pressure. Because the experimental flow rate that is found is in terms of  $\frac{dM}{dt}$ , where M is the mass, and the value needed to solve Darcy's Law is  $\frac{dL}{dt}$ , M has to be converted to  $L$ . This can easily be accomplished by considering that volume and cross sectional area normal to the direction of flow are related via  $L = \frac{V}{A}$ , hence:

$$\frac{dL}{dt} = \frac{dV}{dt} \bigg/ A \quad (2.6.18)$$

Because the complimentary expression for volume uptake would be  $V = M/\rho$ ,  $dV/dt$  can be written:

$$\frac{dV}{dt} = \frac{dM}{dt} \bigg/ \rho \quad (2.6.19)$$

Substituting Equation 2.6.19 into Equation 2.6.18 the flow rate of the moisture front becomes:

$$\frac{dL}{dt} = \frac{dM}{dt} \bigg/ (\rho A) \quad (2.6.20)$$

The equations described above assume total saturation of the medium in which the moisture front advances. However, the laws of capillarity and the structure of the fabric prohibit total saturation to occur, and the flow rate must be adjusted to include fluid filling fraction (Section 2.2). Using Equation 2.6.20 and rejecting the assumption that there is complete filling of the pores, the actual flow rate of the front becomes:

$$\frac{dL}{dt} = \frac{dM}{dt} \bigg/ (\rho A f) \quad (2.6.21)$$

The value found by solving Equation 2.6.21 is the true flow rate and is used for the plot of  $\frac{dL}{dt}$

versus  $\frac{1}{L_o}$ . It should be noted that for a test method to follow this model it must produce a

constant flow rate as well as a constant filling fraction throughout the entire sample. For example, upward wicking tests do not produce a constant flow rate or fluid filling fraction during the entire test due to capillaries dropping out; therefore, the method would not follow this model. Horizontal wicking produces a constant filling fraction but not a constant flow rate due to viscous drag; therefore, the method also can not be applied to the model mentioned above. On



the other hand, a downward wicking test produces a constant flow rate and fluid filling fraction throughout the fabric and may be applied to the postulated model.

Another method to convert the data from mass to length is the normalization of the mass data. This requires a knowledge of the total length of the fabric that the moisture front travels. It will be shown that normalizing the data produces the same flow rate as Equation 2.6.21.

The procedure of downward wicking proposed by Miller can theoretically be used to determine the two fundamental quantities that control the wicking process: capillary pressure ( $P_c$ ) and permeability ( $k$ )<sup>15</sup>. In order for permeability to be solved using this method it has to be assumed that the effective capillary radius remains constant as the height of liquid is increases. This assumption would suggest that saturation, capillary pressure, and permeability are also constants. However, it will be experimentally shown that these properties are not constants, but change as height is varied.

## **Section 2.7 – New Approach to Downward Wicking**

Unlike Miller's approach, a test method that takes into account the variation of permeability and capillary pressure as a function of saturation would more accurately classify the extent of wicking in fabrics. Instead of running the fabrics at a constant angle and changing  $L_o$ , the fabrics are run perpendicular out of the water reservoir and for a fixed horizontal length ( $L_o$ ) before the downward portion of the test. One reason for doing this is because of the difficulty in measuring accurately the angle with which the fabric leaves the reservoir. Duplicating this angle from test to test has been problematic. Second, it should also be mentioned that the water adheres to the underside of the angled fabric near the region of immersion, causing the measured angle to be inaccurate. In contrast, changing the height of the horizontal section above the

reservoir is effortless. Being able to easily change the height allows saturation in the horizontal and downward section to be varied. This method then has the advantage of determining the value of permeability as a function of saturation. In this method the hydrostatic head is easily calculated using:

$$P_h = \rho g h f \quad (2.7.1)$$

where  $f$  is the fluid filling fraction at that height. To solve for permeability using this test method, Darcy's law given in Equation 2.6.7 must be revisited. In order to solve for capillary pressure using Equation 2.2.1, the effective capillary radius at  $f$  must be known. From a knowledge of these variables, permeability can be obtained by:

$$k = \frac{\frac{dL}{dt} L_o \eta}{(P_c - P_h)} \quad (2.7.2)$$

This value of  $k$  is the permeability at the height  $h$  and saturation level  $f$ . By changing the height, one can generate permeability data for a given fabric at almost any level of saturation.

## Section 2.8 - Horizontal Wicking

In many common capillary systems which involve wicking in a substantially horizontal plane, the capillary pressure is much greater than the gravitational force that the latter may be ignored<sup>14</sup>. It has been proposed by many researchers that the flow under capillary pressure in horizontal capillaries can be modeled by the Lucas-Washburn equation<sup>16,21,22,27,28</sup>:

$$L^2 = \frac{\gamma R \cos \theta}{2\eta} t \quad (2.8.1)$$

where  $L$  is the liquid front position or wicking length,  $\gamma$  and  $\eta$  are the surface tension and viscosity of the liquid, respectively,  $\theta$  is the apparent contact angle of the moving front,  $R$  is the

effective hydraulic radius of the capillaries (voids), and  $t$  is time. According to Equation 2.8.1, a plot of  $L$  versus  $t^{1/2}$  should be linear for a given system if the conditions postulated hold. These conditions are 1) that the physical properties of the liquid and the solid remain constant throughout the system; 2) that the driving forces are forces of capillarity; 3) that the radius of the tube or the equivalent radius of the nontubular system is substantially constant; and 4) that the supply of liquid to the system remains adequate<sup>16</sup>. The slope of the plot  $L$  versus  $t^{1/2}$ , which has been called the wicking coefficient  $W_c$ <sup>28</sup> or the rate constant<sup>21</sup>, is given by:

$$Slope = W_c = \left( \frac{\gamma R \cos \theta}{2\eta} \right)^{\frac{1}{2}} \quad (2.8.2)$$

Assuming the test fabric is completely wetted and the contact angle is zero ( $\cos\theta = 1$ ), one can use the wicking coefficient and solve for the effective capillary radius:

$$R = W_c^2 \left( \frac{2\eta}{\gamma} \right) \quad (2.8.3)$$

Equations 2.8.1 thru 2.8.3 assume that the test meets the conditions of a purely horizontal wicking situation as well as saturation of the pores. Since neither of these conditions are met, the wicking coefficient and effective capillary radius solved will be conditional depending on the height that the fabric is raised above the reservoir. Due to capillarity, as height increases, the wicking coefficient, effective radius and the fluid filling fraction decreases. By changing heights, it is possible to solve for wicking coefficients and pore radii at various levels of saturation. Solving for radii at changing levels of saturation becomes increasingly important in a wicking study. These radii can be used to calculate capillary pressure using Equation 2.2.1. and this capillary pressure can then be used to solve for permeability using Equation 2.7.3.

## **Section 2.8 – Combining Downward and Horizontal Wicking**

Three longitudinal wicking tests have been rigorously explained throughout this report. Using a combination of these wicking tests, one can ultimately solve for the two fundamental material properties that control wicking: capillary pressure and permeability. Conducting a horizontal wicking test allows a researcher to calculate the effective capillary radius of a fabric, which in turn can be used to solve for capillary pressure. That capillary pressure can then be used in combination with downward wicking tests and Darcy's law to solve for permeability. These two properties quantitatively help define a fabrics ability to wick moisture.

## Chapter 3

### Experimental Procedure

#### Section 3.1 – Sample Selection and Preparation

Measurements for wicking were conducted on 4 different fabrics, all of which were different in construction. Three of the fabric samples, donated by Milliken, were 100% polyester while the fourth, given by Griffin Manufacturing, was 86% nylon and 14% spandex. Each fabric sample is a color that allows for the visual recording of length as the moisture front advances to premarked distances (i.e. the front can be seen as it flows down the length of the fabric). Table 3.1.1 gives the complete characteristics of the four selected samples.

**Table 3.1.1 – Fabric characteristics**

<b>Sample</b>	<b>Fiber Type</b>	<b>Thickness (cm)</b>	<b>Knit Type</b>
A	100 % Polyester	0.039	Float
B	100% Polyester	0.051	Plain
C	100% Polyester	0.042	Plain
D	86% Nylon/ 14% Spandex	0.070	Plain

The four test samples selected were all classified as weft knit fabrics. Tortora *et al.*<sup>7</sup> defines a weft knit as a fabric in which the “yarns are introduced in a crosswise direction, at right angles to the direction of growth of the fabric, and run or interlock across the fabric.” Sample A is a float stitch, while B, C, and D are characterized as plain stitch fabrics. The construction of a float stitch and plain stitch fabric are depicted in Figure 3.1.1. Although the fabrics appear very similar at the macroscopic level, they are very different in construction. It can be seen by the compound microscope images (Figures 3.1.2 thru 3.1.5) that samples A, B, and C have a very loose and open stitch pattern, while D has a more closed and compact construction.

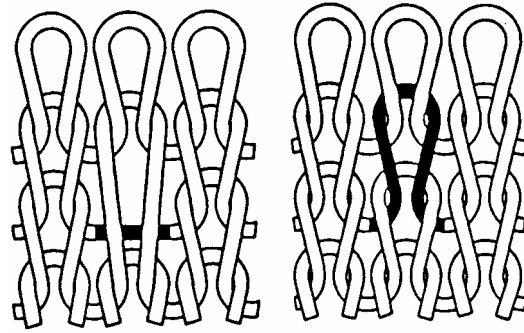


**Figure 3.1.1** – Left: float stitch construction. Right: plain stitch construction.

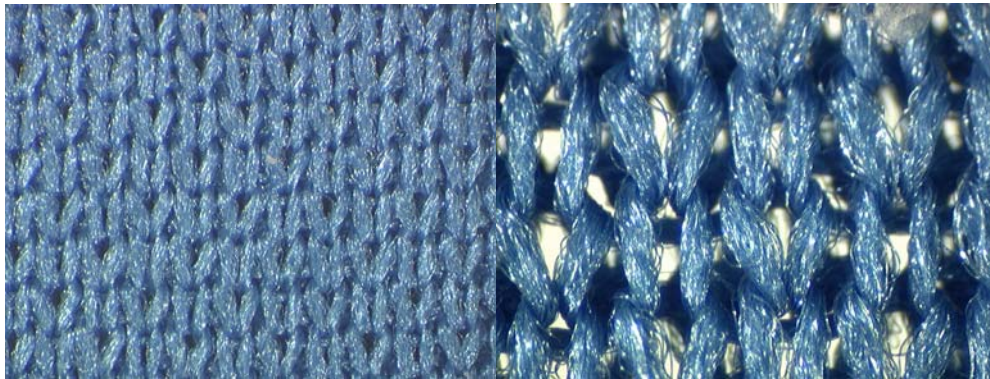


**Figure 3.1.2** – Compound microscope images of the technical face of sample A. The fabric was constructed using 100% polyester yarns in a float stitch pattern. Magnification – left: 16x and right: 40x.

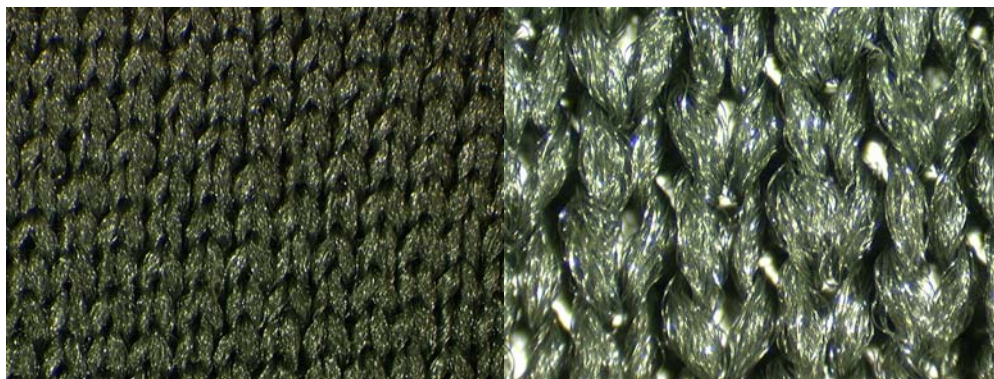


**Figure 3.1.3** – Compound microscope images of the technical face of sample B. The fabric was constructed using 100% polyester yarns in a plain stitch pattern. Magnification – left: 16x and right: 40x.

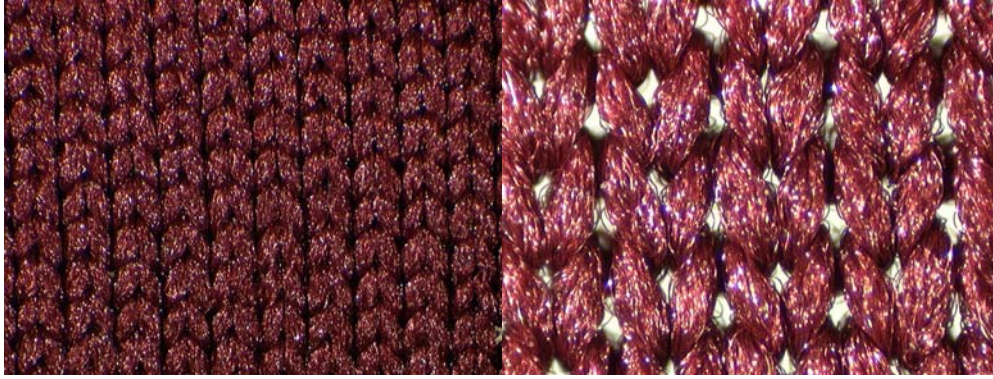


**Figure 3.1.4** – Compound microscope images of the technical face of sample C. The fabric was constructed using 100% polyester yarns in a plain stitch pattern. Magnification – left: 16x and right: 40x.



**Figure 3.1.5** – Compound microscope images of the technical face of sample D. The fabric was constructed using 86% nylon/14% spandex yarns in a plain stitch pattern. Magnification – left: 16x and right: 40x.

The yarns in all the samples are made using synthetic fibers, hence are smooth and have very little hairiness, but the sizes of the yarns appear to be very different. It can be seen from Figure 3.1.3 that the yarns of sample B have little twist and are large in size compared to the smaller yarns of sample A and C. How would these differences in construction impact the moisture wicking characteristics of the fabrics?

The samples were stored at 65% relative humidity before being tested. No additional conditioning, like washing with a surfactant, was done to the fabric samples. The samples were cut in the warp (machine) direction using a one-inch cutting die giving them a width of 2.5 cm.



Preparation of the samples is extremely important. Since knit fabrics are not isotropic, cutting them exactly down the warp direction is critical to moisture flow and reproducibility. Weft direction flow is much slower and can cause the moisture front to flow unevenly through the fabric. The total length of the samples will vary according to which test is being conducted. Distilled water is used as the experimental wicking fluid. Due to the short supply of sample D, not all tests were conducted on this sample.

### **Section 3.2 – Test Apparatus**

Since there is no commercially available test apparatus for wicking, the apparatus had to be constructed. The frame of the apparatus was made using six half-inch stainless steel round bars. Four of the bars were attached to a piece of shelf board using lab frame foots. The other two connected these bars and made up the horizontal wicking area of the apparatus. The wicking area inside the frame was constructed of four quarter-inch stainless steel round bars. The quarter-inch bars are attached to the frame using open-ended rod connectors, which allows for the bars to slide freely through the wicking area. This was done to allow the user to change the length of the test by sliding the bars to the desired location. In order to run downward wicking tests at varying heights, a laboratory jack was used to raise and lower the balance. The round bar used can be found at any local hardware store. A blueprint of the top and side of the apparatus can be seen in Figure 3.2.1.



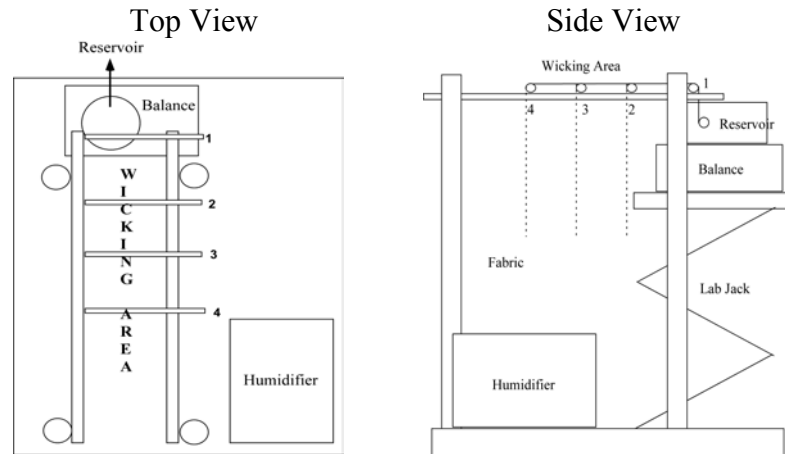


**Figure 3.2.1 – Blueprint of wicking apparatus**

Due to the volatility of water, the apparatus was placed in an environmentally controlled chamber (ECC) made of plexi-glass. The ECC uses a common household humidifier to control the relative humidity, allowing the test to be conducted in a highly saturated condition. This is done in order to minimize the amount of evaporation from the reservoir as well as on the sample itself. The shelf board that supported the apparatus frame was painted with a silicon based waterproof stain in order to keep the wood from absorbing moisture from the surrounding air inside the ECC. Since the moisture regain for the samples tested are very low, the moisture that may accumulate on the fabrics in the ECC is negligible. If the samples contained fibers made of natural sources, the accumulation of moisture due to the relative humidity may alter the results. Due to the size of the ECC, a quarter ton electric hoist was needed to lift the chamber off the apparatus to load the fabric samples.

Since the relative humidity during the time of testing must remain at highly saturated conditions and wicking starts immediately once water comes into contact with the fabric, a method to deliver water to the reservoir without opening the ECC was developed. The task was accomplished by the use of polyethylene tubing and a separatory funnel. The funnel was located

outside the ECC while the connected tubing was positioned perfectly to allow for distilled water to empty into the reservoir. The reservoir sits atop a balance that will be used to determine the mass of water that the sample takes up. The balance is used in order to find the flow rate in terms of mass/time. This is necessary because with most fabrics the human eye cannot easily detect the movement of the moisture front making it is impossible to record the data in terms of length. As mentioned earlier, the fabrics tested for this report were dyed colors that were conducive to visual inspection of the movement of moisture. These fabrics were used in order to see the relationship to the length traveled versus the uptake of mass.

Though it is possible to simply use a stopwatch and record the mass of water uptake at each interval, the balance was connected to a laptop computer with an RS232 cable and used a program called BalanceTalk XL. This program allows for the automation of the process and is designed to read and report the mass uptake as a function of time. With the help of the program, the balance can be zeroed, started and stopped from the computer. This allows for the test to begin and end from the convenience of a computer, all without opening the ECC. The program was told, once initiated, to record the mass at ten-second intervals. The program interface can be seen in Figure 3.2.2.

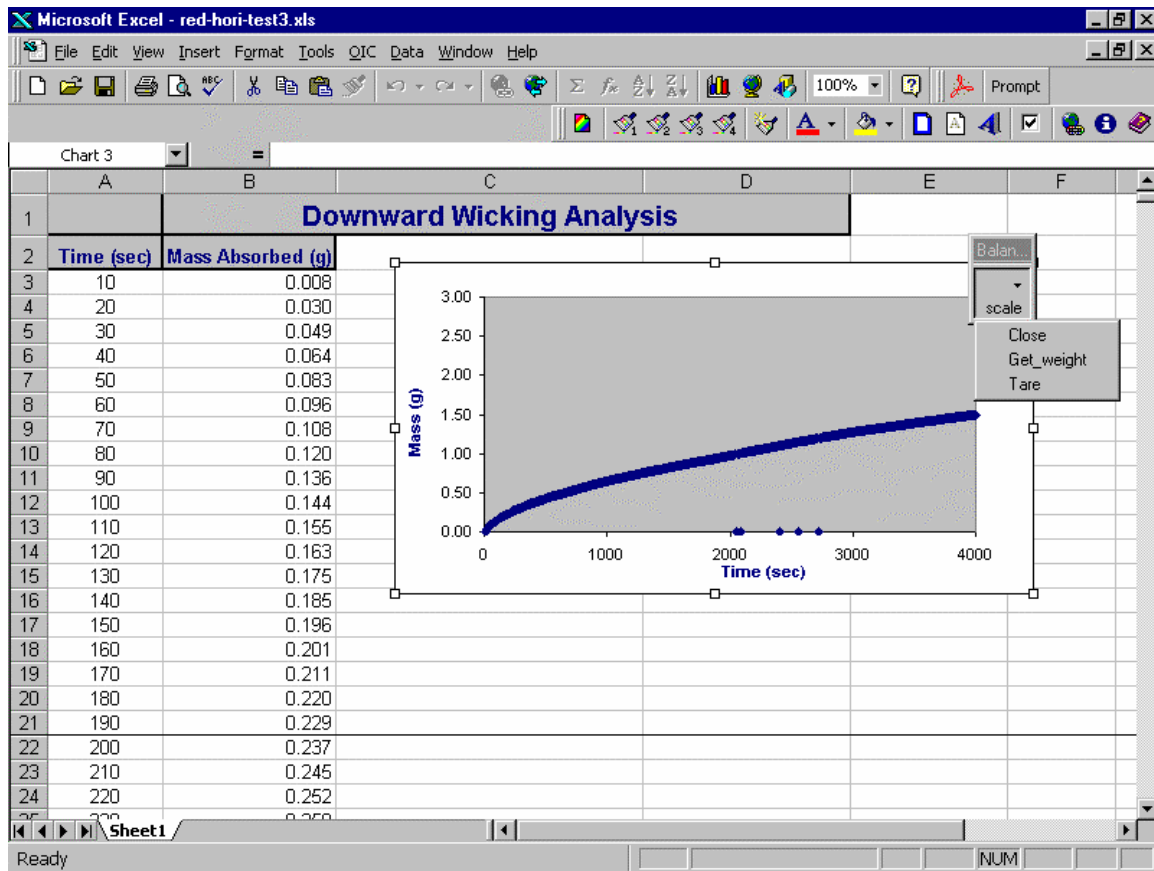


**Figure 3.2.2** – BalanceTalk XL interface for wicking method.

Each test method uses the same apparatus but a different setup. Since each test uses a balance to record mass, the fabric being tested cannot touch any portion of the reservoir. This is because if the fabric is touching the reservoir then the mass recorded will not be accurate due to the added weight of the fabric as well as the weight of the water taken into the fabric. For this reason a “wicking z” was fabricated to immerse the fabric end inside the reservoir without it touching the reservoir. Photographs of the apparatus and its components can be viewed in Figures 3.3.2 through 3.2.10.

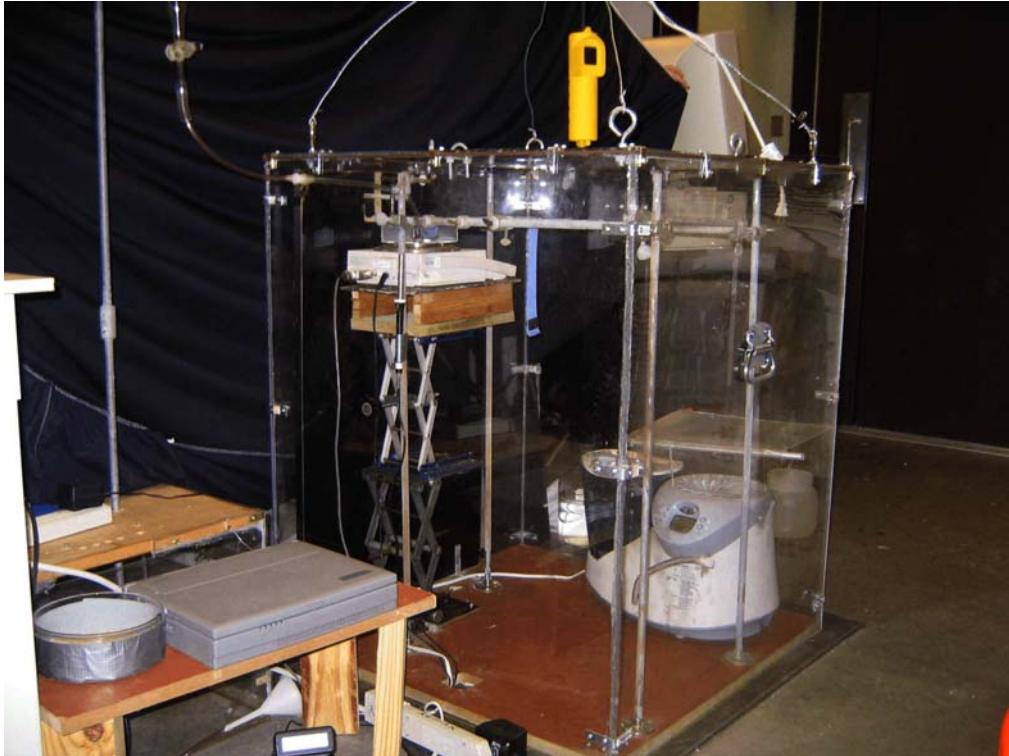


**Figure 3.2.3** – Photograph of apparatus inside the environmentally controlled chamber (ECC).

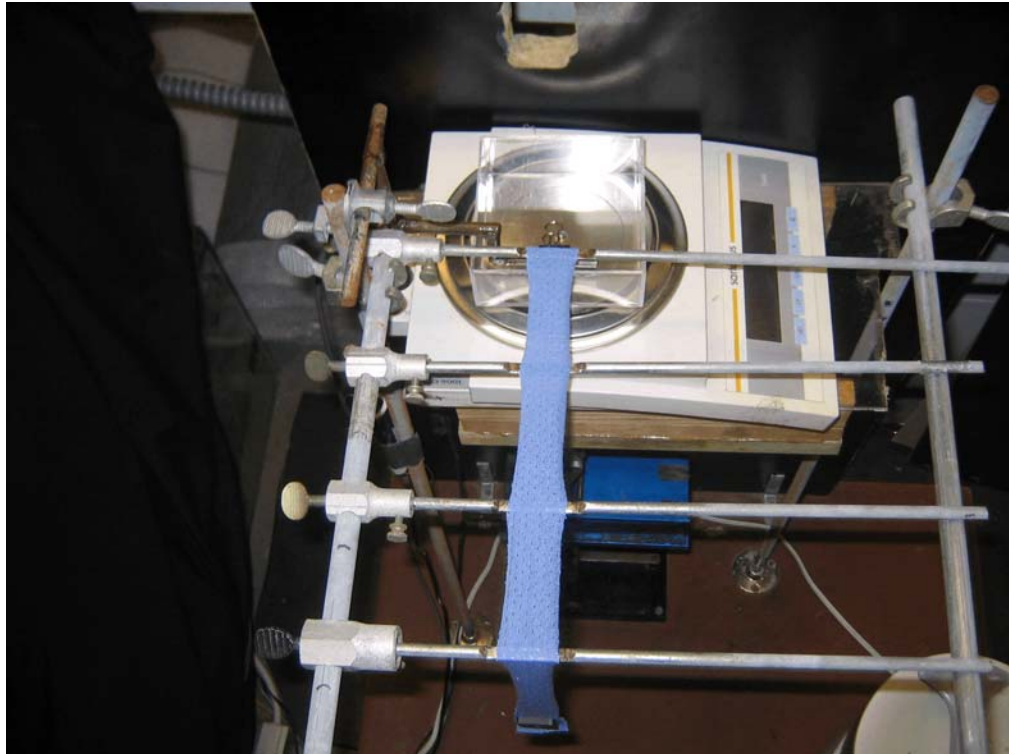


**Figure 3.2.4** – Picture of top view of wicking area.

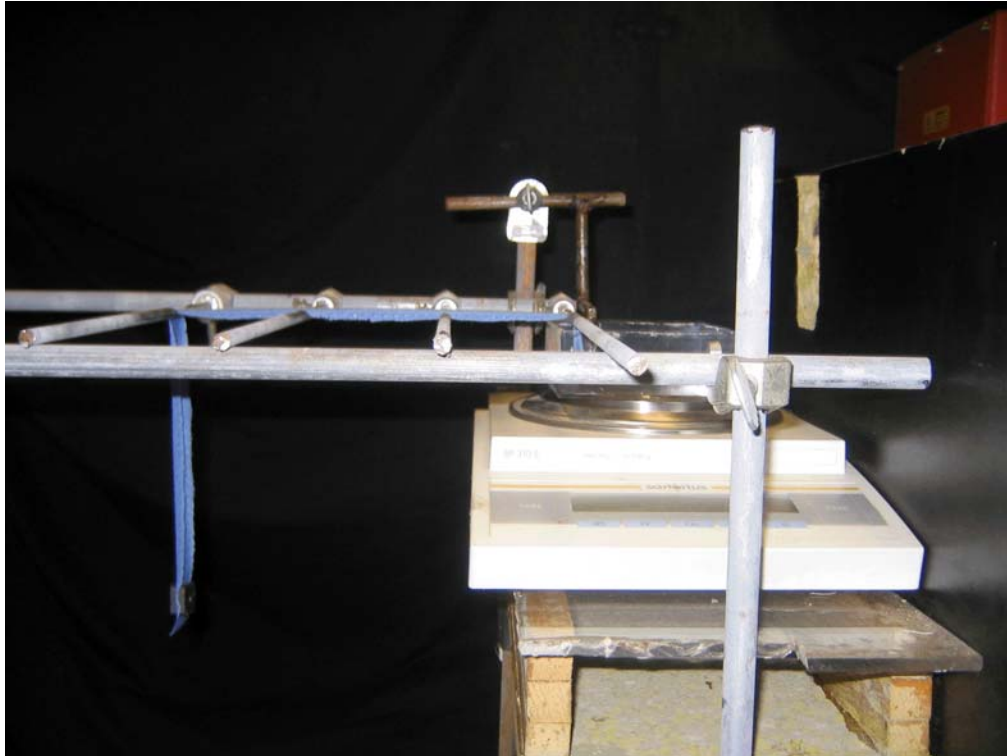


**Figure 3.2.5** – Photograph of side view of wicking area.

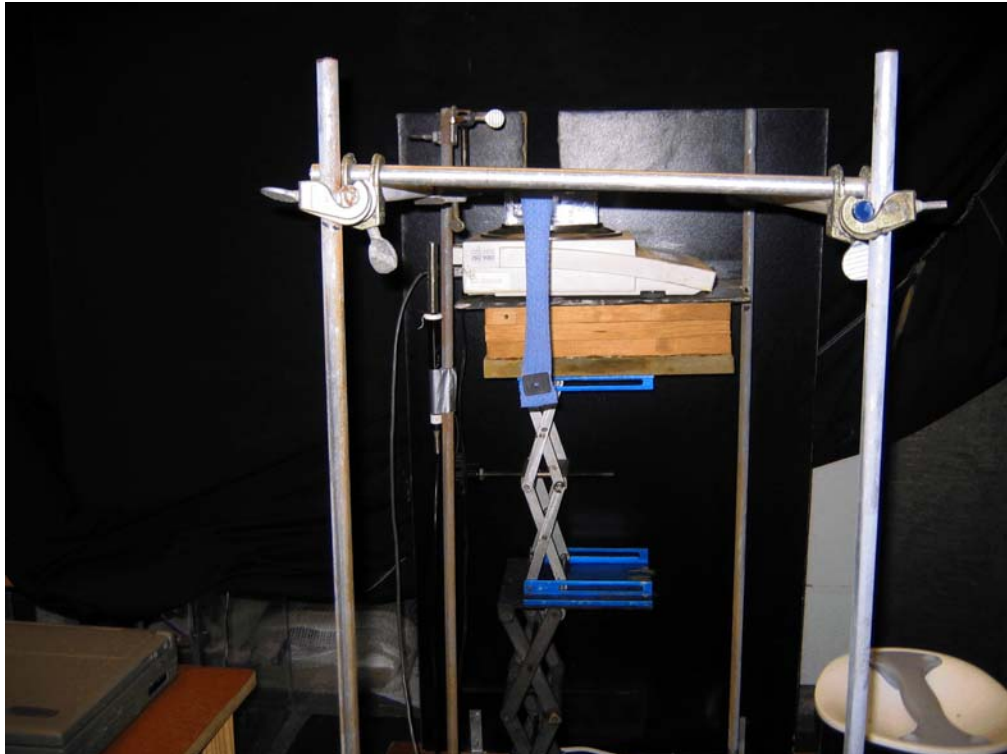


**Figure 3.2.6** – Photograph of front of wicking apparatus.





**Figure 3.2.7** – Picture of wicking z used to immerse fabric inside reservoir.

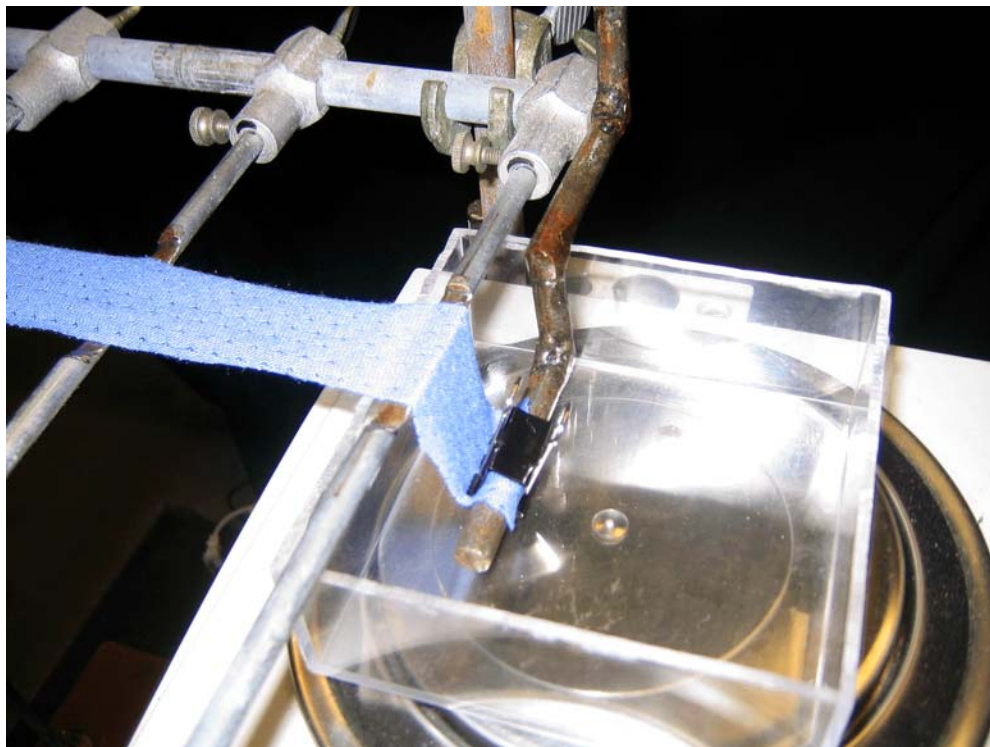


**Figure 3.2.8** – Photograph of sample attached to wicking z inside reservoir. Wicking z allowed fabric to be immersed inside reservoir without touching it.

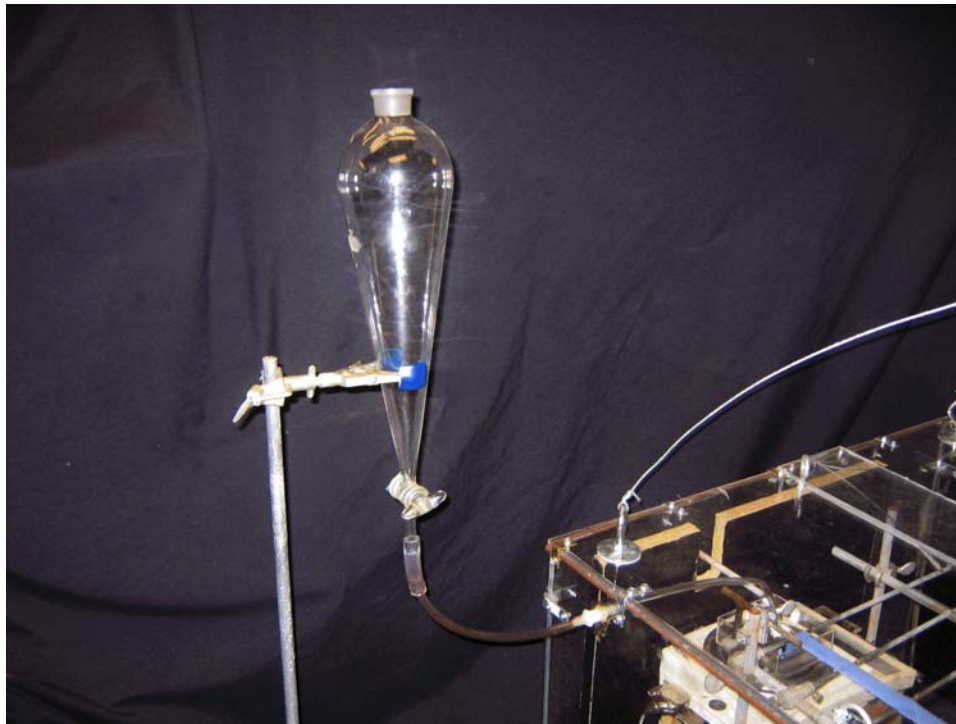


**Figure 3.2.9** – Photograph of separatory funnel which allows water to be delivered to reservoir located in side ECC.

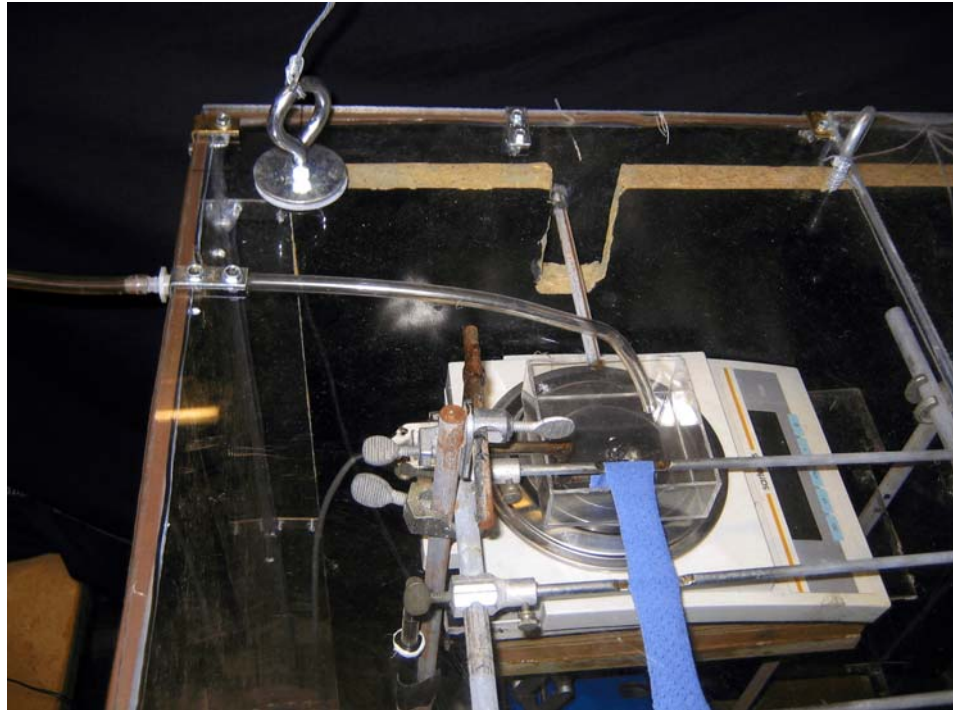


**Figure 3.2.10** – Picture of tubing into reservoir from separatory funnel.

### Section 3.3 – Test Setup and Procedure

For vertical wicking, the scale was not used. The sample was clipped to the wicking z inside the reservoir and run 70 centimeters vertically to one of the wicking bars. Once the sample is in place and the relative humidity is at 90%, the reservoir is filled. Once the reservoir was filled with 250 mL of distilled water wicking started immediately. During the duration of the test, the relative humidity should be kept in the range of 88% to 95%. The test is stopped when the mass uptake becomes constant and the moisture front ceases. This point occurs when the capillary pressure is equal to the hydrostatic pressure. One major drawback to a vertical wicking test is the time constraint. This type of test could take up to a day to run. I ran the tests over night checking to see if the moisture front had ceased the next morning. If it had, I removed the sample and marked where the moisture front had stopped. Using a ruler, I measured and recorded that height to the nearest 0.1 centimeters. The fabric was also weighed and the mass was recorded to the nearest 0.001 grams. The sample was set aside to allow for drying. Once dry, the sample was reweighed. The wet sample mass was subtracted from the dry sample mass in order to record the total water that was wicked. The setup was fairly self-explanatory and can be seen in Figure 3.3.1.

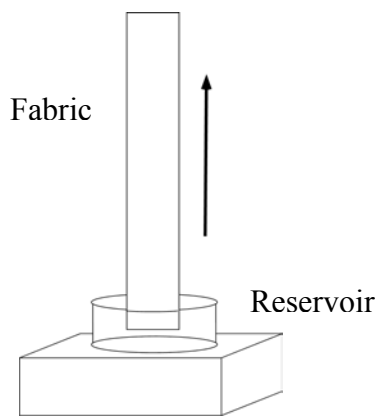


**Figure 3.3.1 – Vertical wicking setup.**



For Miller's downward method, instead of being placed into a bath vertically, the sample and the bath produced an acute angle. Once attached to the wicking z, the fabric was draped over another bar that was connected to a ring stand allowing the fabric to make a  $90^\circ$  triangle. The fabric was kept taut using a load that was placed at the end of the draped portion of the sample. If placed correctly, the sample and the surface of the bath will make an angle that is less than  $90^\circ$ . The reservoir was filled with 250 mL of water from the separatory funnel and the test was started. The test ended when the moisture front reached the load attached to the fabric. The angle  $\beta$  used in this approach was  $30^\circ$ , measured using a protractor and checked by measuring the length and height of the right triangle made by the fabric ( $\sin\beta = \text{height/length}$ ). The angle was kept constant as the  $L_o$  values were changed to 8, 10, 12, 14.5, and 17 cm, respectively. Miller's test setup was shown in Section 2.6 as Figure 2.6.1.

For reasons explained earlier, a new approach to solve for permeability was developed. The new approach consists of using horizontal wicking to solve for capillary pressure and downward wicking to solve for the complimentary permeability. Though it is possible to run both tests separately, a method was developed to run them in series. The proposed test method is simply a horizontal-downward wicking test. First, the fabric, contradictory to Miller's method, is run perpendicular out of the reservoir to bar 1 as seen in Figure 3.3.3. Then the fabric is run horizontally throughout the wicking area for 20 centimeters where it is draped over bar 4. It is a good idea to move the other test bars to equal distances throughout the wicking area. The placement of the test bars keeps the soaked fabric from drooping, therefore, not compromising the horizontal integrity of the sample. After being draped over bar 4, the fabric is hung vertically down for 55 centimeters. The load is attached to the end of the fabric sample. Once in place, the fabric was marked using a permanent marker where horizontal wicking would start (i.e., where it

touches bar 1). The fabric was removed and 2-cm increments were measured and marked down the fabric starting at that mark and ending at 70 centimeters. That means that downward wicking was recorded to 50 centimeters. The fabric was then placed back to its original position. Once in place, the ECC was closed and the humidifier turned on. 250 ml of distilled water was measured out using a beaker and poured into the separatory funnel. At a relative humidity of 90%, the testing was ready to begin. The separatory funnel was emptied into the reservoir and wicking began. The scale was zeroed and the computer initiated once the moisture front reached bar 1 signaling the start of horizontal wicking. At the same time, a stop watch was also started in order to record the time it took the moisture to travel from mark to mark. This was done in order to compare length versus time data to that of the normalized data. The test concluded once the front reached the last mark on the downward section of the fabric.

To solve for a range of permeabilities at varying saturation levels, the test was repeated at numerous vertical heights above the water line. The heights tested were 1.5, 2.5, 3.5, and 4.5 centimeters, respectively. Three repeats were done for each fabric at each height. It should be noted that sample C was run using a horizontal length of 12 centimeters due to the slow wicking behavior. The sample was also a dark red color which made it very difficult to see the moisture flow at slow rates. The differences in  $L_o$  does not make a difference in the final outcome due to Darcy's law taking into account the horizontal length. This can be concluded by the linearity of the best fit line in the plot of flow rate versus  $L_o$  as seen in Figure 3.3.2.

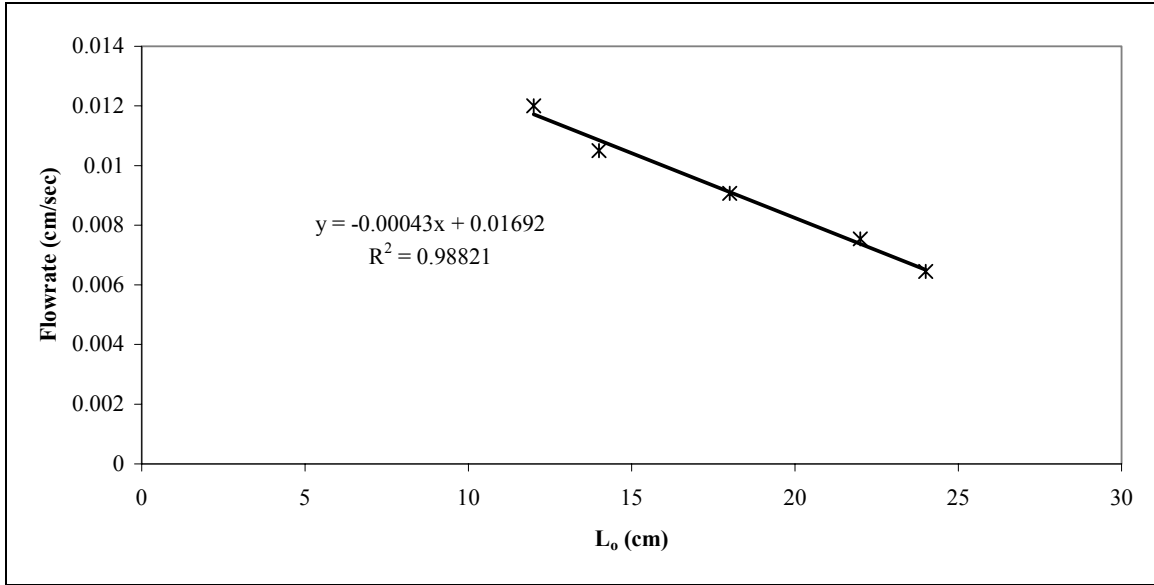


**Figure 3.3.2** – Plot of flow rate versus  $L_o$  using sample D at a vertical rise of 1.5 cm. The linearity of the line proves that the choice of  $L_o$  is arbitrary in solving Darcy's law.

The plot shown in Figure 3.3.2 demonstrates how the choice of  $L_o$  becomes arbitrary in order to solve Darcy's law when conducting horizontal-downward wicking tests. Figure 3.3.3 shows the setup used to conduct horizontal-downward wicking tests.

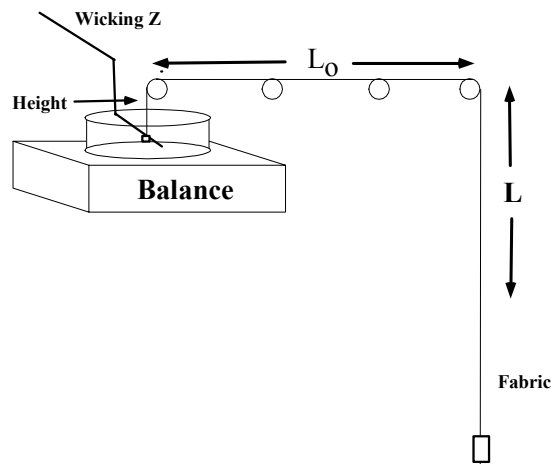


**Figure 3.3.3** – Arrangement for carrying out horizontal-downward wicking method

Every test was run at a temperature of  $21 \pm 2$  °C and relative humidity of  $90 \pm 2\%$ . The load used to keep the fabric taut during each of the test weighed 8.5 grams. The load was just

magnets placed on both sides of the fabric. It should be noted that a significant amount of weight may affect the final outcome due to the added tension. If too much weight is used, it could close some of the capillaries and inhibit fluid flow through the fabric.

After the termination of a horizontal-downward wicking test, the fluid filling fraction of the fabric was calculated. The volume of the fluid ( $V_{\text{fluid}}$ ) can be calculated by one of two methods. The first method requires cutting a piece of the tested fabric where moisture migrated during the wicking portion of the test. Weigh the wet section of the fabric and record the mass of water that was taken into the fabric. Let the fabric completely dry and weigh the dry fabric sample. With those masses and Equation 2.2.3,  $V_{\text{fluid}}$  can be calculated.

The second method requires the wicking test to be conducted using a balance. If a balance is used to record the mass of fluid uptake during wicking, then  $M_w - M_d$  is equal to the final mass recorded before termination of the test. To solve for the volume of the fabric, one needs to calculate the length, width, and thickness of the sample. The former two are easily measured using a ruler, while measuring the thickness of a fabric may be quite tedious. In most cases a close guess may be accomplished using calipers or a compressometer. I used digital calipers and recorded the thickness to the 0.001 cm.

Once all variables are known, the total volume was easily calculated using  $V_{\text{total}} = \text{width} \times \text{length} \times \text{thickness}$ . With  $V_{\text{fluid}}$  and  $V_{\text{total}}$  now known, Equation 2.2.2 was used to solve for the fluid filling fraction ( $f$ ). The latter of the two methods was the chosen approach used in this thesis. The main reason is because moisture can evaporate or transfer while cutting and weighing a wicked section of fabric. That would indicate a lower reported  $f$  value and inaccuracy in the calculations.

## **Chapter 4**

### **Results and Discussion**

Before wicking tests were conducted, many conditions and assumptions were put to rest. They included the effect of relative humidity on wicking tests using distilled water, the fluid filling fraction phenomenon, the assumption of a constant flow rate during downward wicking, and how a fabric reacts to distilled water compared to liquid perspiration. The constants for water are listed in the Symbols and Abbreviations section of this thesis.

#### **Section 4.1 – Effects of Relative Humidity**

Testing laboratories require the atmosphere to be maintained at  $65 \pm 2\%$  RH and  $20 \pm 2$  °C in order to carry out accurate physical testing of textiles<sup>25</sup>. Because of the volatile nature of water, 65% relative humidity would allow evaporation to skew the results. It is not generally acknowledged that, with a significantly volatile liquid such as water, evaporation from the wet surface of the fabric can compete with the capillary process that advances the liquid front. To eliminate fluid evaporation from our analysis, we carried out wicking tests inside a saturated, enclosed environment. Many researchers have run similar wicking tests with less volatile liquids such as hexadecane, but in order to understand the effects of perspiration on a performance fabric, water makes for a much better choice for such tests.

When considering the effects of atmospheric moisture on textile materials, the important quantity is not how much moisture the air already holds, but how much more it is capable of holding. This factor governs whether fibers will lose moisture to or gain moisture from the atmosphere. The capacity of the atmosphere to hold further moisture is calculated by taking the maximum possible atmospheric moisture content at a particular temperature and working out

what percentage of it has already been taken up. This quantity is known as the relative humidity (RH) of the atmosphere. It is important to note that the relative humidity of the atmosphere changes with temperature even when the total quantity of water vapor contained in the air remains the same. Figure 4.1.1 below shows how a beaker of water tested at a RH of 65% loses mass over time due to evaporation, while a beaker of water left at a RH of greater than 85% does not.

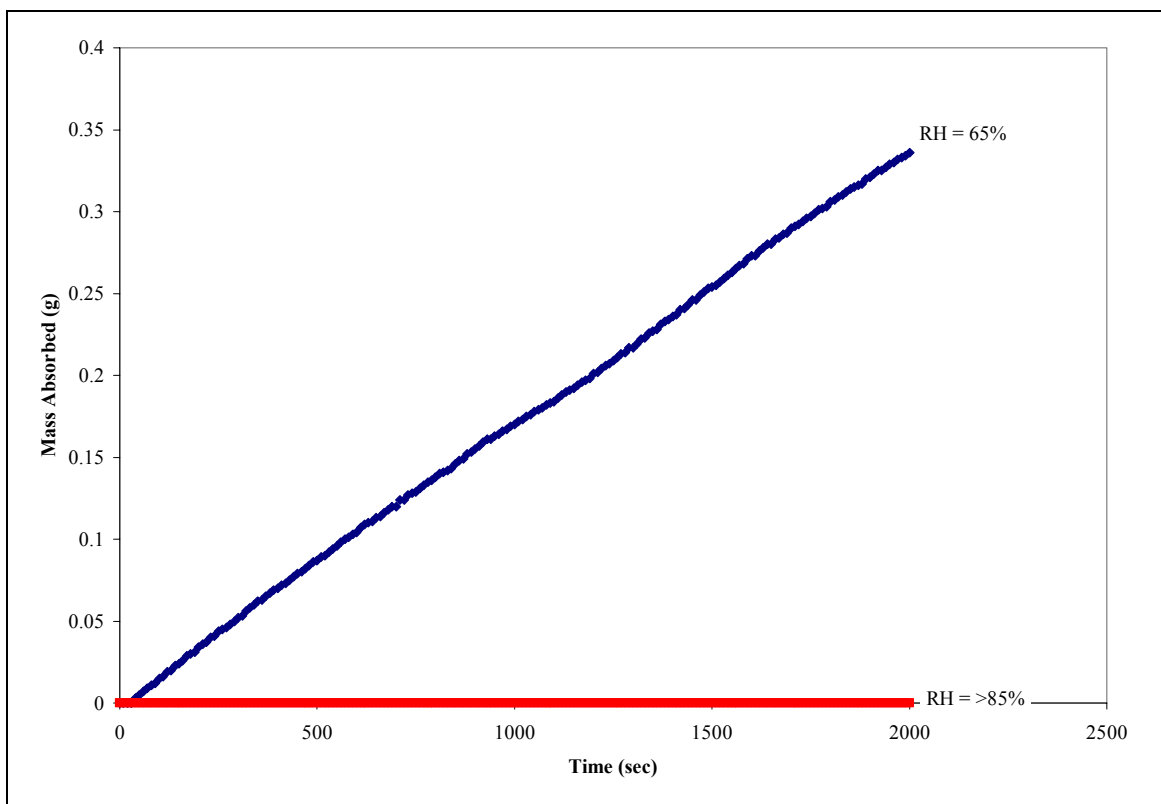


**Figure 4.1.1** – Effect of relative humidity on a beaker of water at a temperature of 22 °C.

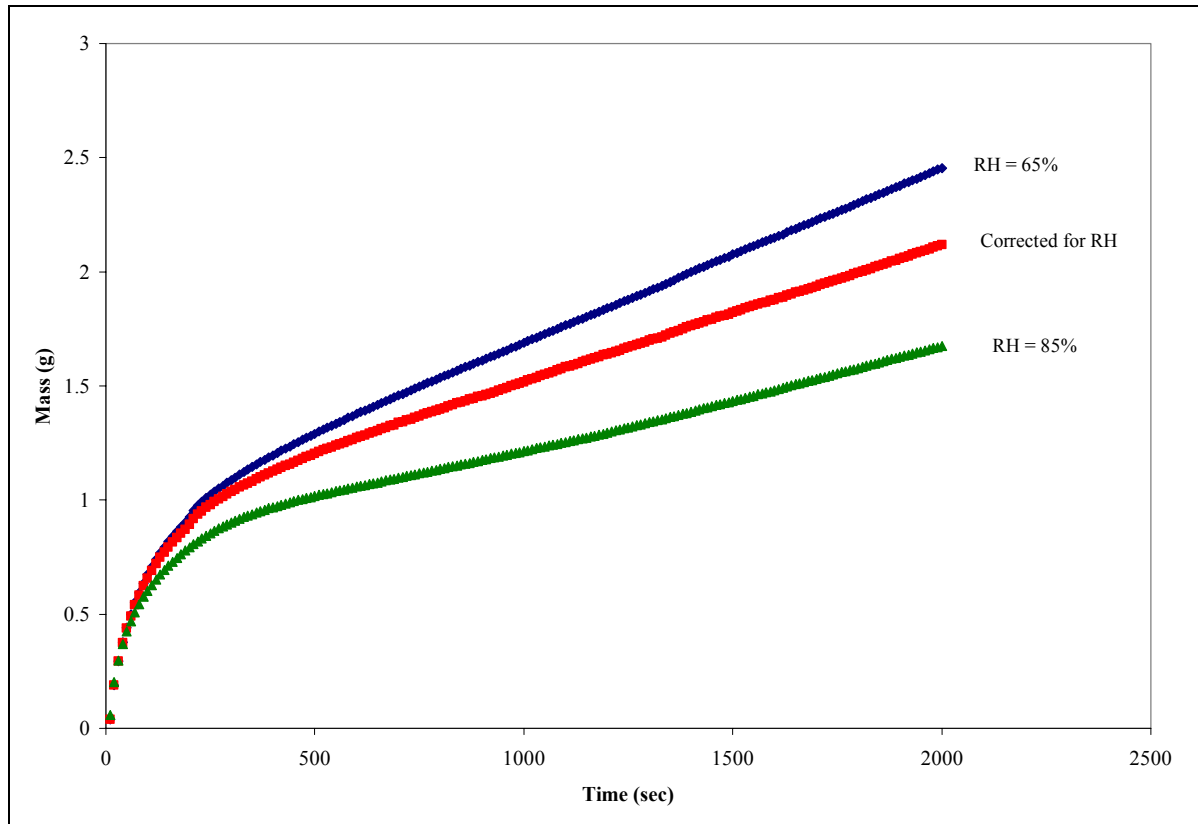


**Figure 4.1.2** - The effects of relative humidity on the results obtained using sample D when conducting a downward wicking test. The temperature was maintained at 22 °C.

It can be seen in Figure 4.1.2 that the evaporation of water under low RH conditions will significantly change the recorded flow rates found for a given sample. All tests were done at a temperature of 21°C +/- 1°C. The lower the RH the higher the flow rate becomes as one can see by the difference in the slopes of the two curves. The slope of the curve for the sample run at a RH of 65% is  $7.700 \times 10^{-4}$  g/sec, while the slope of the curve for the sample run at a RH of 85% is  $4.380 \times 10^{-4}$  g/sec. Figure 4.1.2 also shows the plot of the downward wicking test at a RH of 65% subtracted from the data accumulated during the beaker test at a RH of 65%. If evaporation of fluid from the reservoir is the only factor affecting the increase in flow rate, the corrected line should equal that of the slope of 85% relative humidity line. The slope of the corrected line, as seen in the figure above, is  $6.027 \times 10^{-4}$  g/sec, proving that evaporation from the dish is not the

only cause of increasing flow rates. A simple explanation for this phenomenon is that at low RH values more water can evaporate from the fabric itself causing the pores to dry faster allowing more water to flow from the reservoir onto the fabric. Because these fabrics are designed to dry rapidly, the reason above may take place even in a short period of time. It should be noted that these tests were run using the downward wicking approach of Miller and are only used to show the role that relative humidity plays on the results of wicking tests that use water. The slopes of these lines were taken after the 500 second mark, which indicated downward wicking.

#### **Section 4.2 – Wicking Comparison of Distilled Water versus Perspiration**

It has been reported in the literature that the use of a less volatile liquid like hexadecane can be used for testing the wicking of a fabric or yarn. Since the tests conducted here are used to describe the interaction of a performance fabric when in contact with body perspiration, distilled water was used to best simulate human sweat. The principle electrolytes in sweat include sodium, chloride (sodium chloride is table salt) and potassium (potassium chloride is often marked as a table salt substitute). Most human sweat contains at least 700 milligrams of sodium per liter, and probably averages around 1000 milligrams of sodium per liter<sup>29</sup>. In order to simulate sweat, a saline solution was produced. Sodium chloride (NaCl) has an atomic mass of 58 g/mol with the sodium atom occupying 40% of that mass; therefore, 1 gram of sodium per liter equals 2.5 grams of NaCl per liter. Converting volume to milliliters, the solution becomes 0.0025 g NaCl/ml or a 0.25% solution. This solution was used in a horizontal-downward wicking test with a height of 1.5 cm and a horizontal length of 7 cm on sample D. To compare the results obtained by the perspiration simulant, distilled and tap water were also used following the same test method. The results can be seen in Figure 4.2.1.



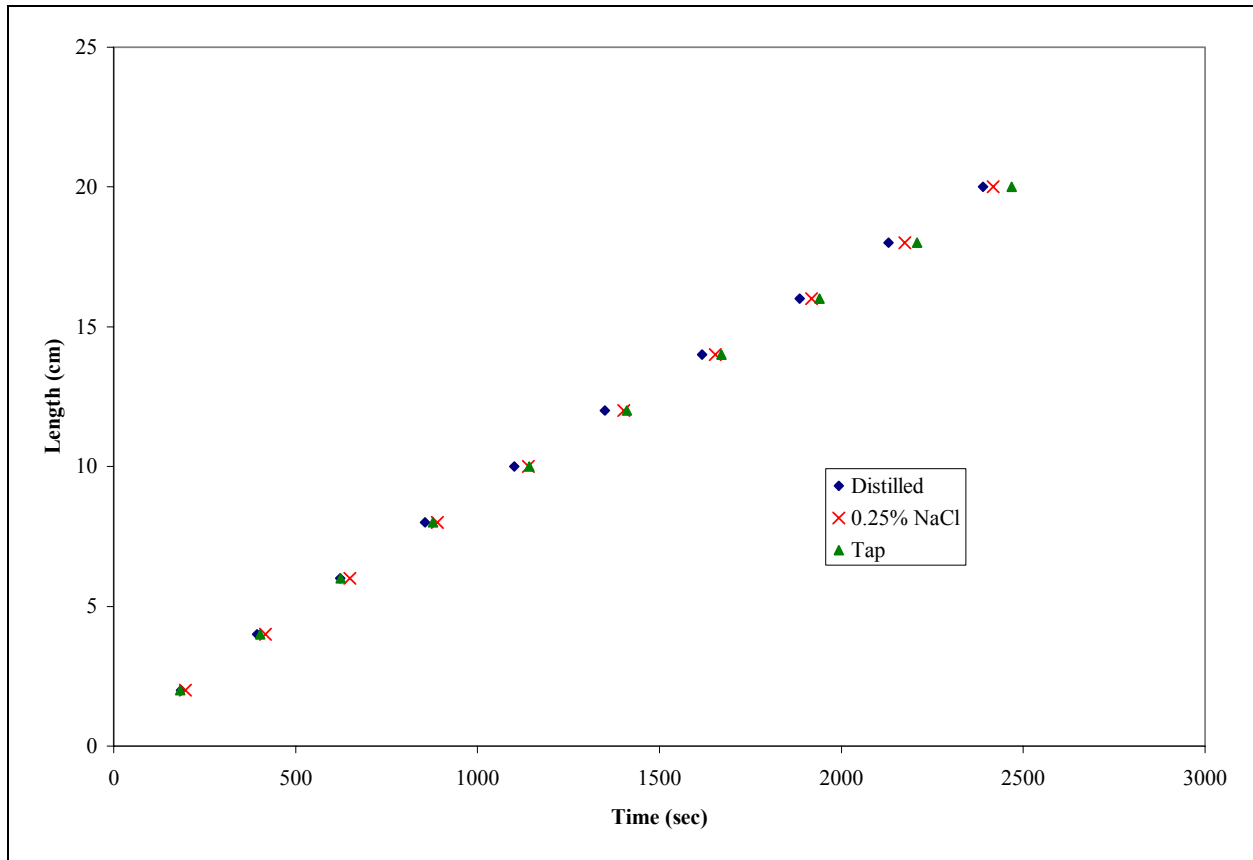


**Figure 4.2.1** – Downward wicking comparison using distilled water, tap water, and a sweat simulant as wicking fluid.

As seen by Figure 4.2.1 above, testing with distilled water is a good indication of how a fabric would act when in contact with liquid perspiration. The slope of the distilled water line is 0.0082 cm/sec, while the slope of the simulant and tap water lines are 0.0081 and 0.0079 cm/sec, respectively.

### Section 4.3 – Reproducibility of Test Results

When a material is tested, certain requirements are expected from the results. The most important and implicit requirement from a test method is that it is reproducible. The true accuracy of a test method can only be gauged by repeated testing of the material<sup>25</sup>. Most textile materials have variability when it comes to their physical properties, with natural fibers having

the most variation in their properties<sup>25</sup>. The problem of variability in a material can be dealt with by the proper selection of representative samples and the use of suitable statistical methods to analyze the results. Due to variability of a fabric, the values obtained by a test method are not expected to be exactly the same, but are expected to fall within an accepted spread of values. Wicking tests of the nature described earlier are no different and data collected from such tests should be reproducible. Before tests begin, reproducibility should be investigated. In order to test the reproducibility of the horizontal-downward wicking method, three repeats of test 1 (height of 1.5 cm), were conducted using samples A, B, and C. The results can be seen graphically in the figures below. It should be noted that a different strip of the sample fabric was used for each trial.

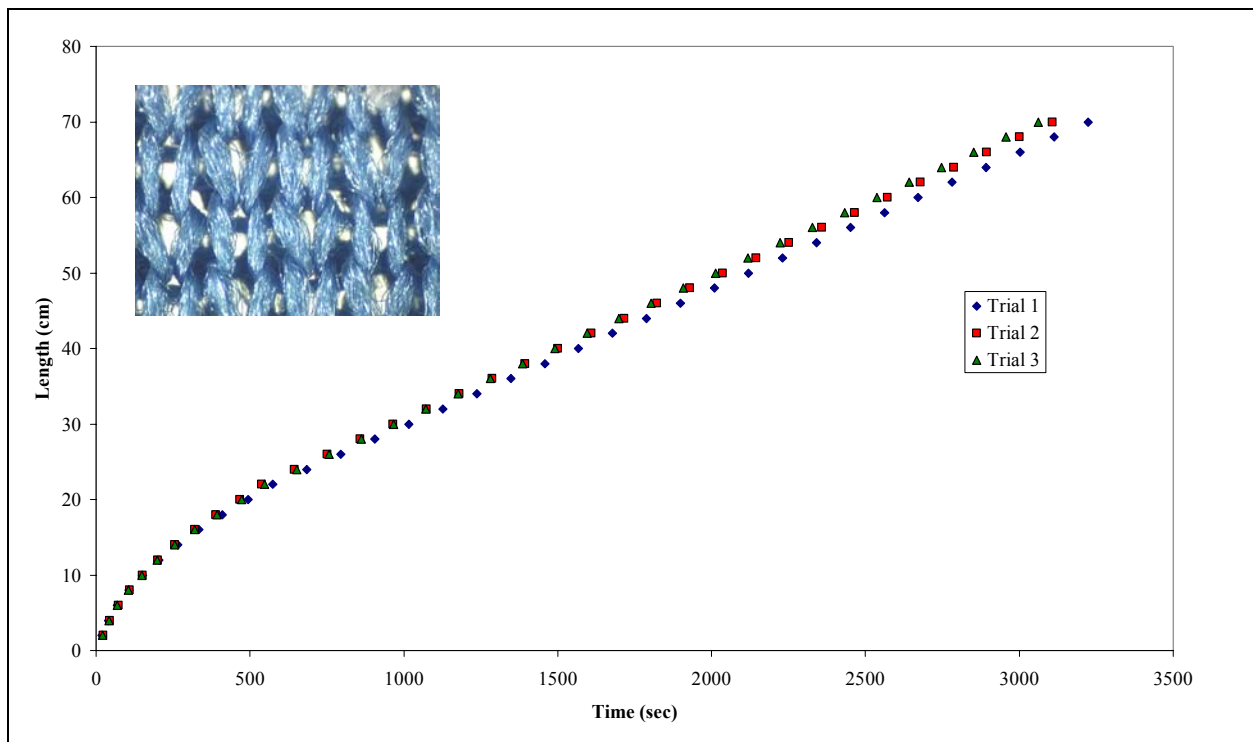


**Figure 4.3.1** – Three repetitions of a horizontal-downward wicking test using sample A. The test was conducted at a height of 1.5 cm and a horizontal length of 20 cm.

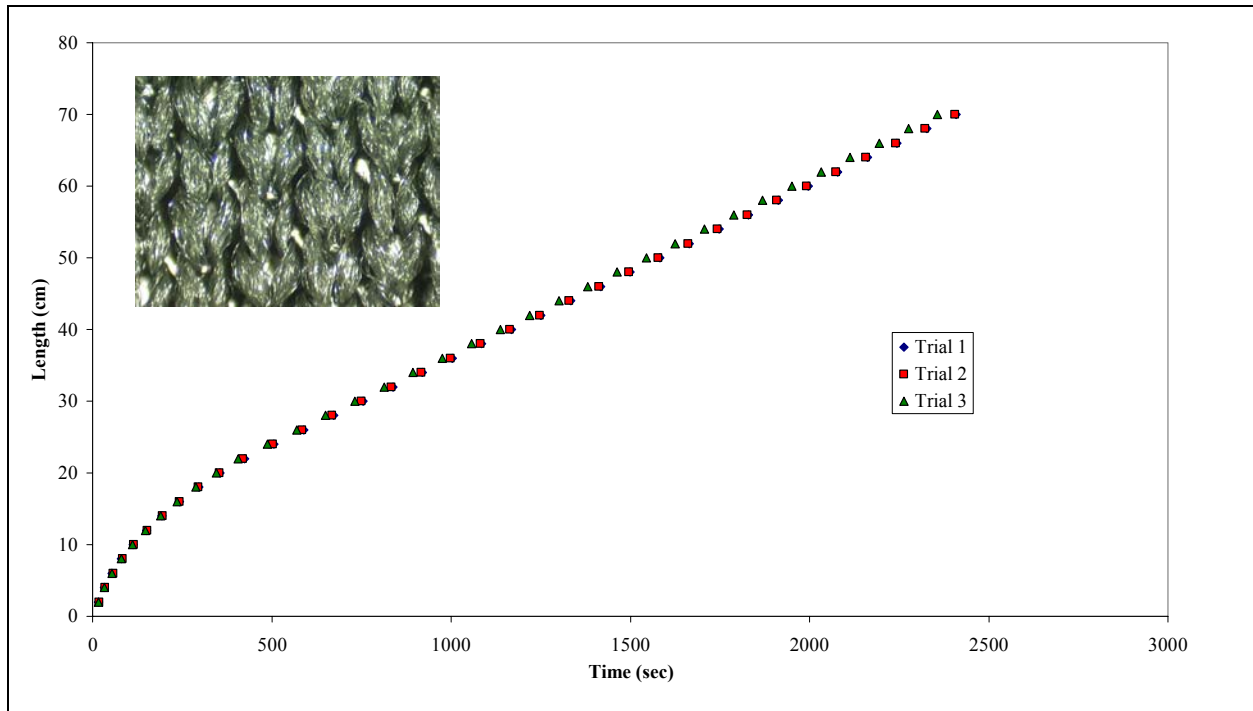


**Figure 4.3.2** – Three repetitions of a horizontal-downward wicking test using sample B. The test was conducted at a height of 1.5 cm and a horizontal length of 20 cm.

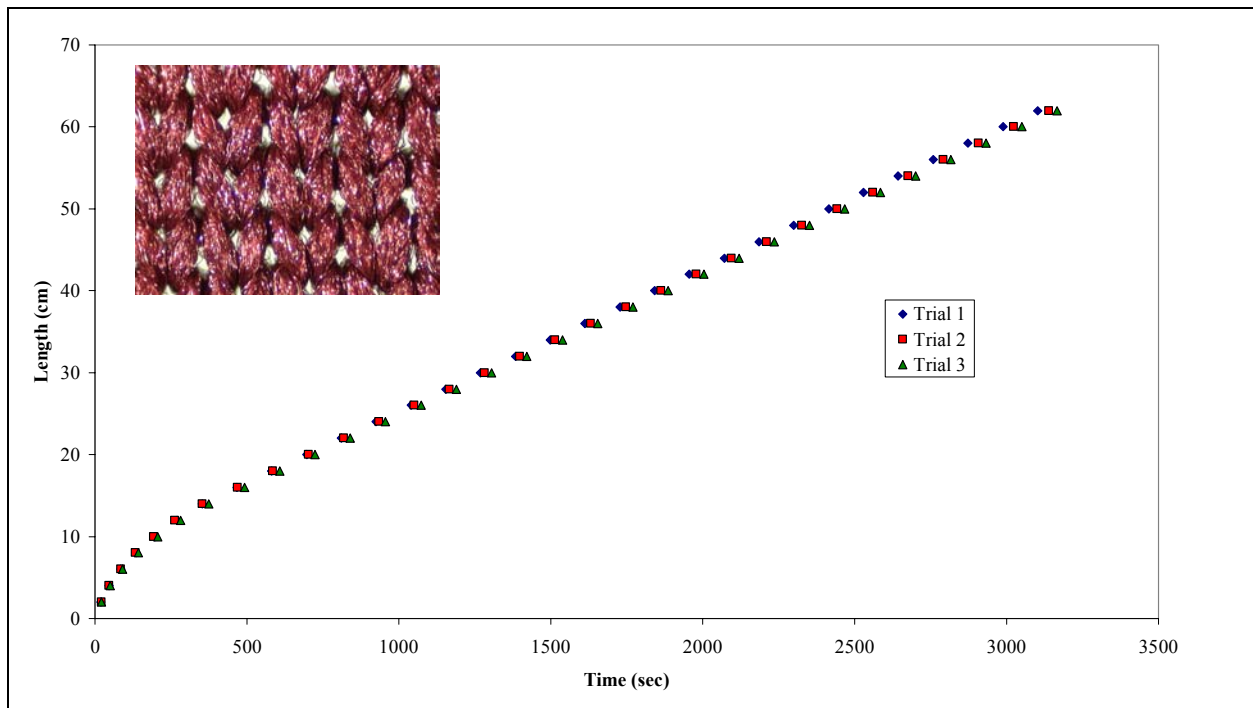


**Figure 4.3.3** – Three repetitions of a horizontal-downward wicking test using sample C. The test was conducted at a height of 1.5 cm and a horizontal length of 12 cm.

As demonstrated by Figures 4.3.1 through 4.3.3, the tests are reproducible for every sample. As explained earlier, preparation of the samples becomes increasingly important when talking about reproducibility. If the samples are not cut in the right direction, the data may be misleading. Due to the slight variability, every test conducted was done three times and the values reported are the averages of those tests.

#### **Section 4.4 – Normalizing Data**

As mentioned in Section 2.5, the data collected from the balance is in terms of mass versus time, when the models for wicking require the data to be in terms of length. Using the fluid filling fraction and Equation 2.6.21 is one way for solving for the needed values. An alternative method is to normalize the mass data collected to the length of the test. This method requires knowing the exact length of the fabric that the moisture travels during the entire test. With the total length  $L_{total}$  of the fabric tested known, the mass  $M$  at any time can be normalized using:

$$L = \frac{L_{total}}{M_{total}} M \quad (4.4.1)$$

where  $L$  is the solved length and  $M_{total}$  is the total mass of the moisture held within the fabric. To validate this method a test using sample A was conducted following the procedure stated in Section 3.3. The test was run earlier in the study and only the downward portion of the results is shown in Figure 4.4.1.

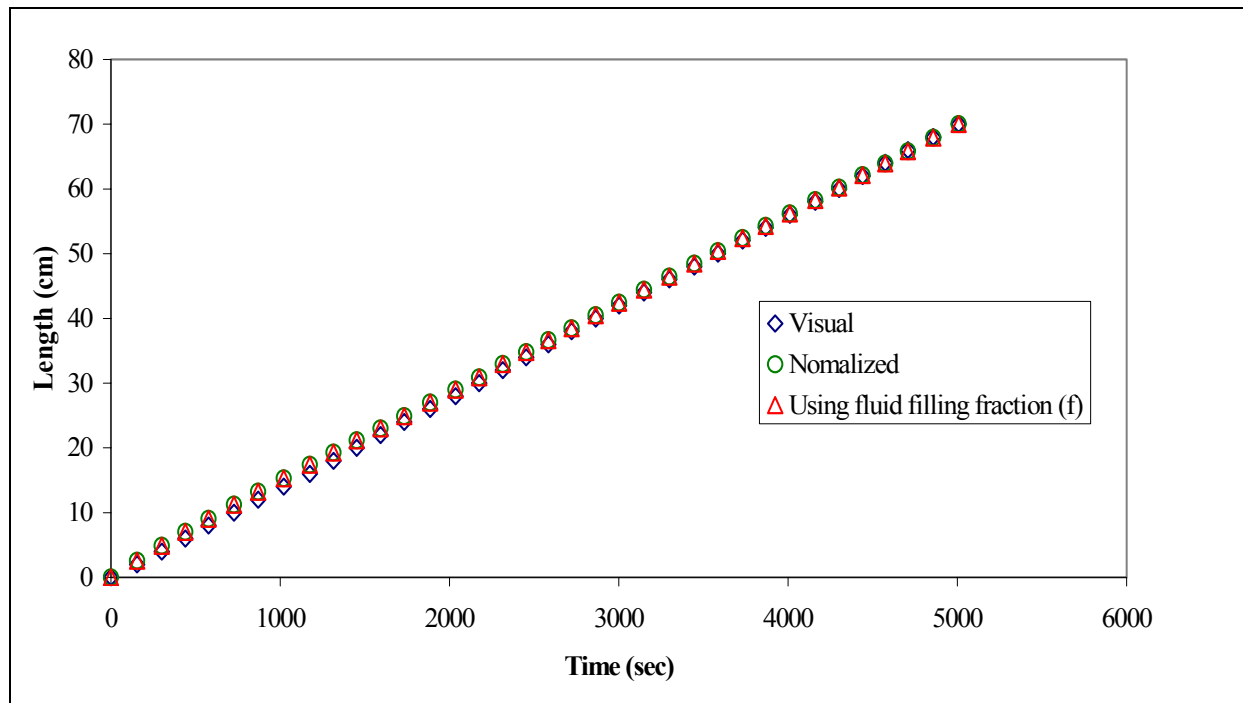


**Figure 4.4.1** – Comparison of various ways to analyze wicking data. Visual ( $\diamond$ ) refers to data recorded by watching moisture front as it traveled along fabric sample. Normalized ( $\circ$ ) refers to mass data obtained by balance and computer program that were normalized using Equation 4.4.1. Using fluid filling fraction ( $\Delta$ ) refers to the method for solving length using Equation 2.6.21.

As seen by Figure 4.4.1, the three methods used to analyze wicking data will generate the same information. Visual refers to the method where the moisture front was physically watched and the time was recorded as it passed premarked distances on the fabric. The slope of the line referred to as visual is 0.0140 cm/sec, while the slopes of the lines for the normalized and fluid filling fraction data are 0.0138 cm/sec. With this known, these types of tests can be run with fabrics that do not allow for visual inspection of moisture movement. These tests can be conducted using any fabric in conjunction with a balance and a computer program as long as the final length of the flow is known.

## Section 4.5 – Fluid Filling Fraction

It has been proposed that as height increases the amount of moisture held in the fabric decreases. This happens because of the fabric's porous make-up and the laws of capillarity that govern fluid flow. What about when the flow is in the horizontal or downward direction? Does the fluid filling fraction stay constant throughout the fabric? At first one might not think that it does due to the slowing of the moisture front during horizontal wicking, but that is not the case. The moisture front does slow because of viscous drag, but the moisture still fills the appropriate capillaries throughout the fabric. Figure 4.5.1 shows the fluid filling fractions at 2-cm increments throughout sample D. The fluid filling fractions were determined using Equation 2.2.2. The test setup included a height of 1.5 centimeters, a horizontal length of 18 centimeters, and a downward length of 18 centimeters.

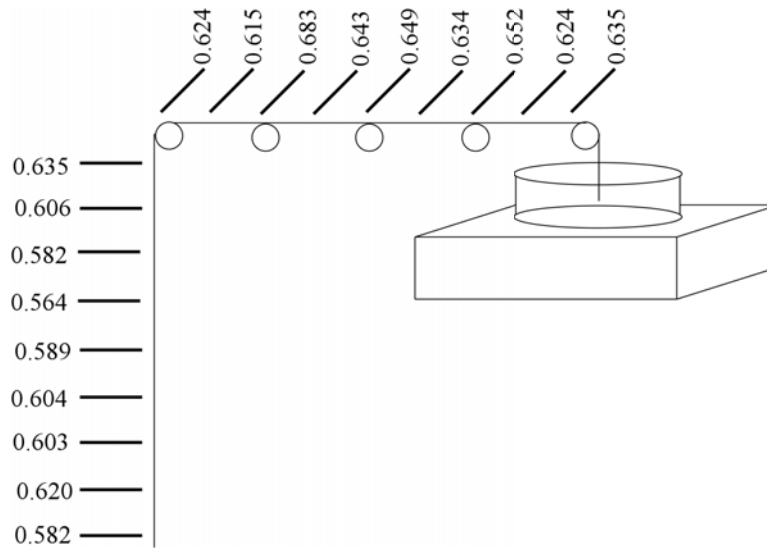


**Figure 4.5.1** – Fluid filling fractions in 2-centimeter increments of sample D. The height of the test was 1.5 cm.

The average filling fraction in the fabric was 0.617 with a standard deviation and a coefficient of variance of 0.029 and 4.77%, respectively. It can be concluded that the saturation

level in a fabric at a given height remains essentially constant when the flow is in the horizontal and downward direction; therefore, permeability and capillary pressure are presumed to also be constant.

#### Section 4.6 – Constant Flow Rate during Downward Wicking

Dr. Bernard Miller proposed a test method to solve for the ability of a fabric to wick moisture that was based on the physics behind a siphon (Section 2.6). In general, as moisture begins a downward descent, the flow rate of the front would become essentially constant. This was checked by running sample D using a vertical rise of 1.5 centimeters, a horizontal length of 24 centimeters, and a downward length of 18 centimeters. The results of the test were observed visually and can be seen graphically in Figures 4.6.1 and 4.6.2.

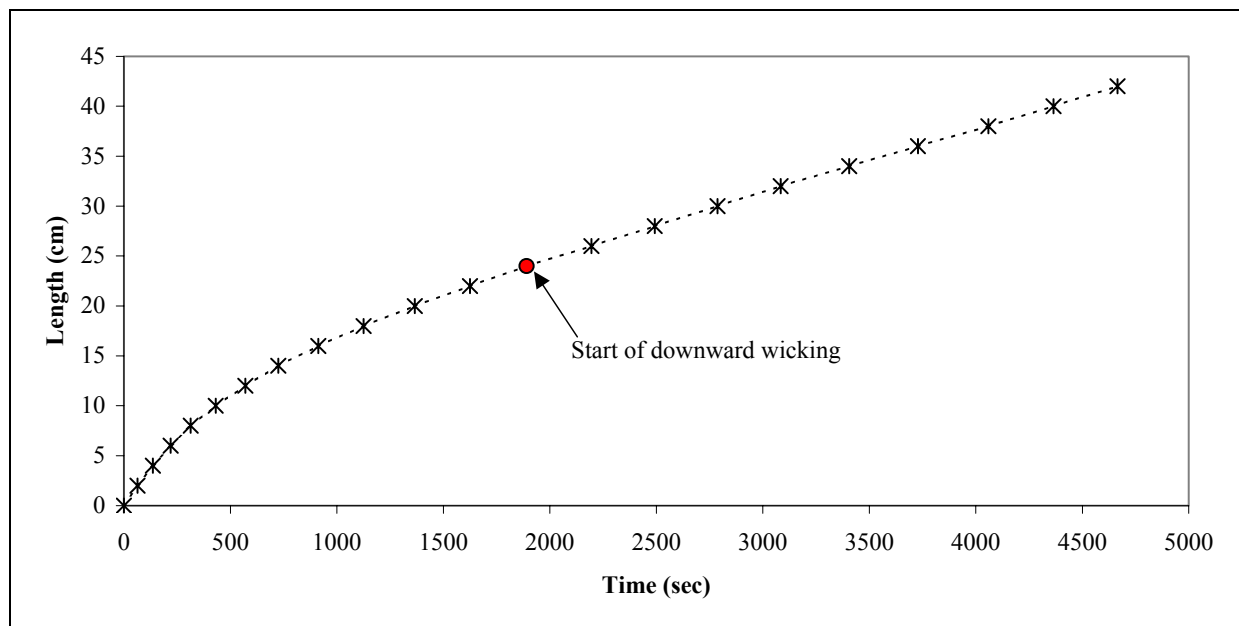


**Figure 4.6.1** – Plot of length versus time for a horizontal-downward wicking test using sample D. Data was obtained by visual inspection of the moisture. Dot indicates the start of downward wicking.

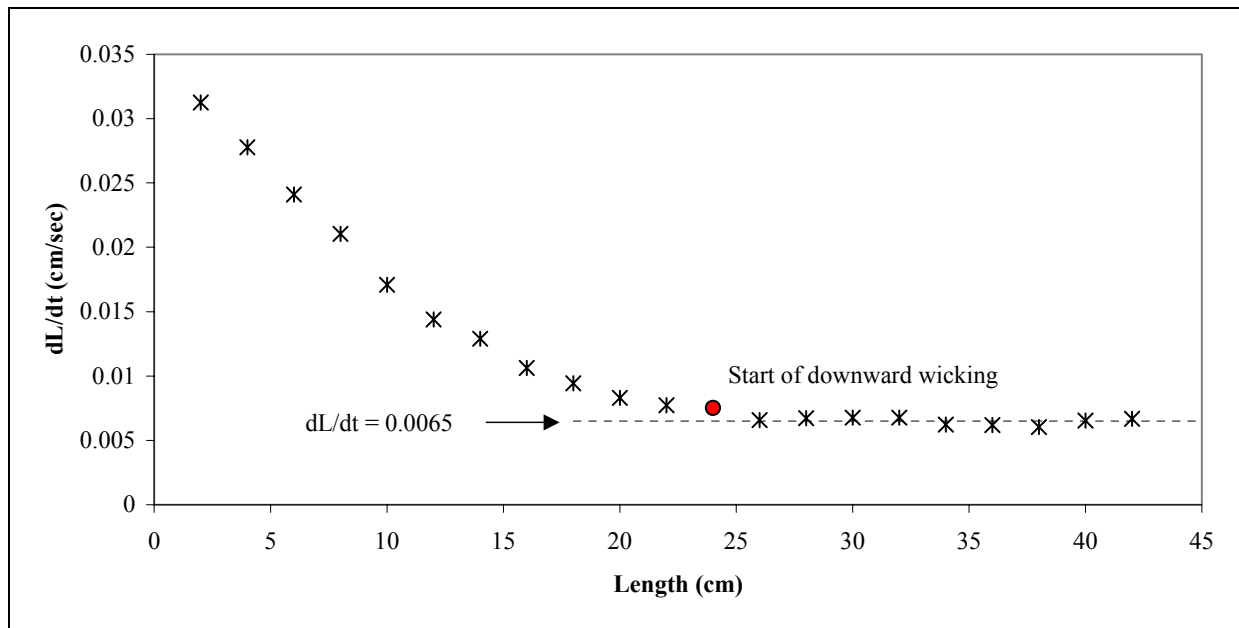


**Figure 4.6.2** – Plot of flow rate versus length for a horizontal-downward wicking test using sample D. Dot indicates start of downward wicking.

The flow rate data given in Figure 4.6.2 demonstrate how wicking, after initial deceleration during the horizontal segment of the test, remains essentially constant for the downward portion of the test. The dot on both figures indicates the start of downward wicking. The average flow rate is 0.0065 cm/sec with a standard deviation and coefficient of variance of 0.0003 and 4.21%. This proves that Miller's theory of a constant downward flow rate does work; therefore, downward wicking can be used in conjunction with Darcy's law to solve for permeability.

## Section 4.7 – Vertical Wicking Results

The results of vertical wicking tests for samples A, B and C are presented in Table 4.7.1. Looking at the results it can be seen that sample C raised to the greatest height with sample B and A following. With that information known and under the theories of capillarity, sample C would presumably have the smallest effective capillary radius, leaving sample A with the largest.



**Table 4.7.1 – Results of vertical wicking tests**

<b>Sample</b>	<b>Height Raised – <math>L_c</math> (cm)</b>	<b>Mass of Moisture Uptake (g)</b>
<b>A</b>	48.5	1.0168
<b>B</b>	51.5	1.7680
<b>C</b>	58.7	1.7775

As stated in Section 2.5, vertical wicking tests, based on numerous assumptions, may produce capillary pressure as well as capillary radius data using the LaPlace equation. Using Equation 2.5.4 the capillary radii of the test samples were calculated and are reported in Table 4.7.2 below. In order for these calculations to be accurate, it must be assumed that capillary pressure is a constant and not a function of saturation or that saturation stays the same as height is increased. It will be shown, however, as height increases, saturation decreases. Due to this reasoning, capillary pressure would not remain constant, but increase as fluid flows from the larger voids to the smaller ones.

**Table 4.7.2 – Solutions to LaPlace equation for vertical wicking.**

<b>Sample</b>	<b>Capillary Radius <math>R</math> (<math>\mu\text{m}</math>)</b>
<b>A</b>	30.63
<b>B</b>	28.84
<b>C</b>	25.31

Again, the data in Table 4.7.2 show sample A having the largest capillary radius and sample C having the smallest. Later in the report it will be shown that sample B has the largest pore radius at a given height. According to this method, sample C would be the best wicking fabric of the group, which again will be shown later to be false. One reason sample A wicked moisture to the lowest height may be due to its structure and not pore size distribution. The float stitch fabric has less yarn intersections, which has been reported to act as new reservoirs that feed the remaining branches equally<sup>16</sup>. With the decreased number of reservoirs, the water could

not climb to the same heights as the rest. This also shows that a vertical wicking test produces misleading information based on the fact that it does not take into account fabric structure.

#### Section 4.8 – Results for Downward Wicking as Proposed by Miller

Miller's approach to downward wicking, as seen in Section 2.6, was tested using sample D. The results can be seen in Table 4.8.1 below. It is understood that as  $L_o$  increases, the height that the moisture must travel also increases if  $\beta$  is kept constant. That would explain the drop in the fluid filling fraction, as well as a decrease in flow rate with increased  $L_o$  values. For reasons explained earlier, it is no surprise that the highest saturation and fastest flow rate are observed for the shortest  $L_o$ , 8 cm.

**Table 4.8.1** – Downward wicking results using approach proposed by Miller

Test	$\beta$	$L_o$ (cm)	$dM/dt$ (g/s)	$A$ (cm <sup>2</sup> )	$f$	$dL/dt$ (cm/s)
1	30°	8	0.00158	0.1455	0.563	0.0193
2	30°	10	0.00115	0.1455	0.502	0.0158
3	30°	12	0.00087	0.1455	0.457	0.0130
4	30°	14.5	0.00062	0.1455	0.411	0.0103
5	30°	17	0.00056	0.1455	0.376	0.0102

The mass flow rates were found using the graph produced from BalanceTalk XL and the fluid filling fractions ( $f$ ) were calculated using Equations 2.2.2 and 2.2.3. With  $dM/dt$  and  $f$  calculated, it was easy to then solve for the flow rate in terms of length versus time ( $dL/dt$ ) with the help of Equation 2.6.21. After these values were calculated, Miller's derivations of Darcy's law to solve for permeability and capillary pressure were tested. Miller suggests that a ratio of flow rates can be used in order to solve for these variables as seen in Equation 2.6.13. If Miller's theory holds true, then any combination of  $L_o$  values and their correlating flow rates would give the same values for the desired information. Below, in Table 4.8.2, are the solved values of

Equations 2.6.13, 2.6.15, and 2.6.16. The first column defines what  $L_o$  combination was used. For example, the term 8,10 means that the data from Table 4.8.1 for the tests using an initial length of 8 and 10 cm were used to solve for the ratio  $F$ .

**Table 4.8.2** – Solutions for permeability using ratio of flow rates.

Tests	F	$L_c$ (cm)	$k$ (cm <sup>2</sup> - using $dL/dt_1$ )
8,10	1.225	44.5	$6.360 \times 10^{-8}$
8,12	1.482	156.8	$1.920 \times 10^{-8}$
8,14.5	1.873	-104.9	$-3.059 \times 10^{-8}$
8,17	1.884	31.1	$8.782 \times 10^{-8}$
10,12	1.210	-130	$-2.520 \times 10^{-8}$
10,14.5	1.529	-48.5	$-7.244 \times 10^{-8}$
10,17	1.538	28.2	$9.473 \times 10^{-8}$
12,14.5	1.264	11.9	$1.747 \times 10^{-7}$
12,17	1.271	15.9	$1.427 \times 10^{-7}$

As seen by the data in Table 4.8.2, putting two flow rates from this type of test into a ratio in order to solve Darcy's law does not give reproducible solutions. Therefore, an inaccurate characterization of permeability would be obtained by using this method. These irreproducible results are most likely due to the incorrect assumption that permeability is a constant throughout tests with changing heights. It can also be concluded that the choice of  $L_o$  to run this type of downward wicking test becomes arbitrary. Due to this flaw in Miller's approach, a second method was proposed and tested. It included arranging Darcy's law such that it followed the form  $y = mx + b$  as seen in Equation 2.6.17. To solve for permeability using that form of the equation requires the plotting of flow rate ( $dL/dt$ ) versus the associated  $L_o$  values. The graphical representation of this postulation can be seen in Figure 4.8.1. The equation of the best fit line as well as the  $R^2$  value is also given in the figure.

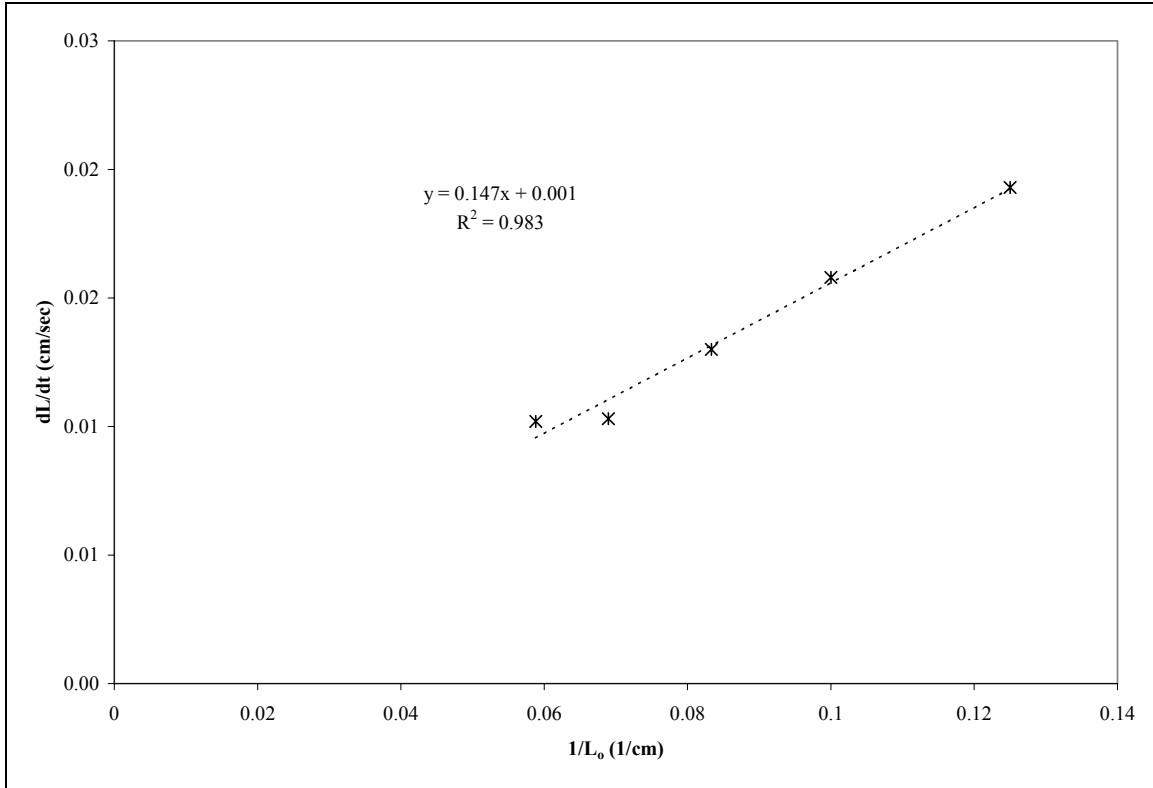


**Figure 4.8.1** – Plot of  $dL/dt$  versus  $1/L_0$  for sample D using Miller’s downward wicking method.

The best fit line seems to offer a reasonable linear relationship with an  $R^2$  value of 0.983. If that is the case, then permeability can then be solved using Equation 2.6.17 where the slope of the line ( $m$ ) and the y-intercept are equal to  $\frac{\rho g k L_c}{2\eta}$  and  $\frac{\rho g k}{2\eta}(1 - \sin \beta)$ , respectively. Using a y-intercept value of 0.001 and a slope of 0.147, permeability ( $k$ ) and  $L_c$  were found to be  $4.082 \times 10^{-8}$  darcys and 72.9 cm, respectively. These answers seem reasonable, but earlier in the study it was found that some samples exhibited negative y-intercepts. A negative intercept would produce a negative permeability, which would lead to a negative  $L_c$  value. Figure 4.8.2 graphically demonstrates a sample that exhibits a negative y-intercept. The sample used for the test was Coolmax polyester from DuPont.

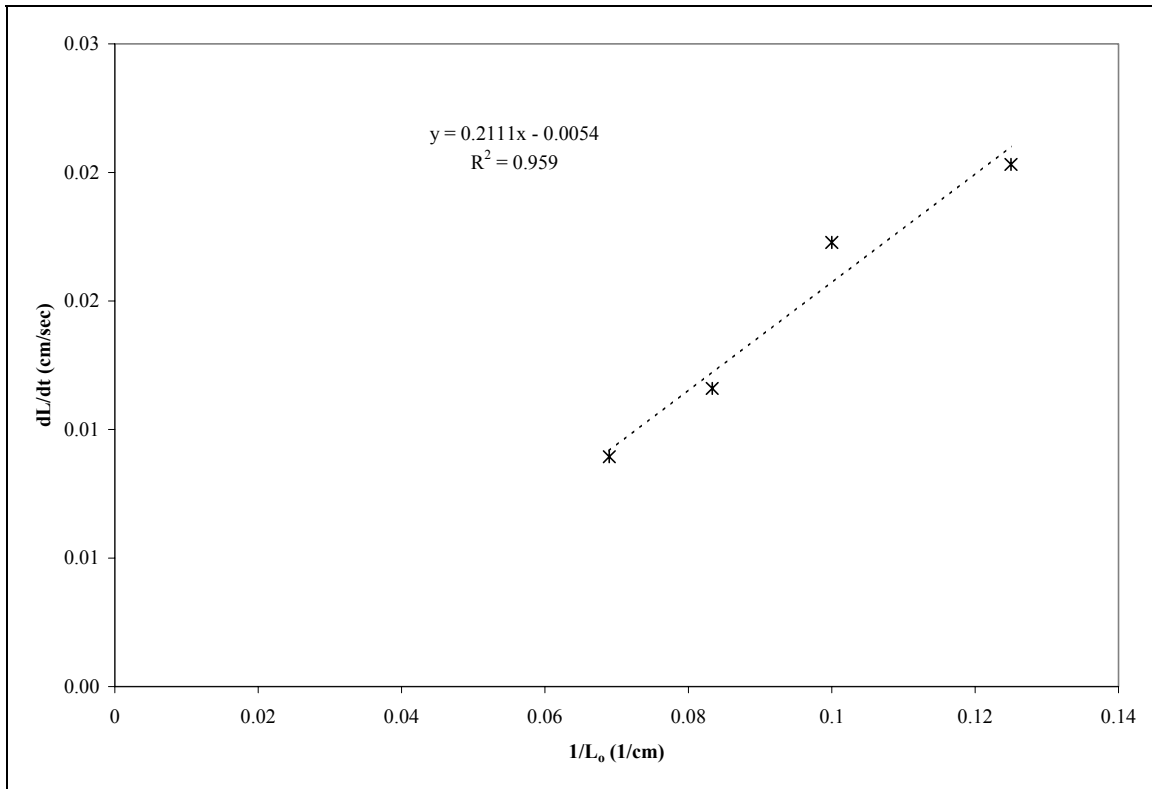


**Figure 4.8.2** – Downward wicking results for Coolmax polyester using Miller’s method.

Again, it is demonstrated that using this method essentially produces a linear relationship between the two variables. One notices, however, that the equation for the best fit line contains a negative y-intercept. The negative y-intercept would produce a negative permeability, therefore, providing evidence how the same testing can produce erroneous results. The fluid filling fractions for each test dropped as the height was increased, just as one would predict. They were 0.678 for a  $L_o$  of 8 cm, 0.629 for a  $L_o$  of 10 cm, 0.452 and 0.270 for  $L_o$ ’s of 12 and 14.5 cm. This sample proves that the method does not produce useful permeability information for all fabrics. Again, it needs to be reiterated that permeability and capillary pressure are not constants, but change as saturation changes.

## Section 4.9 – Horizontal-Downward Wicking Test Results

The results from the horizontal-downward wicking tests are presented in Figures 4.9.1 through 4.9.3. The vertical heights for each test are also shown. It can be seen that as the vertical height above the reservoir is raised, the flow rate of the moisture front slows. This phenomenon, as predicted, happens in all the samples.

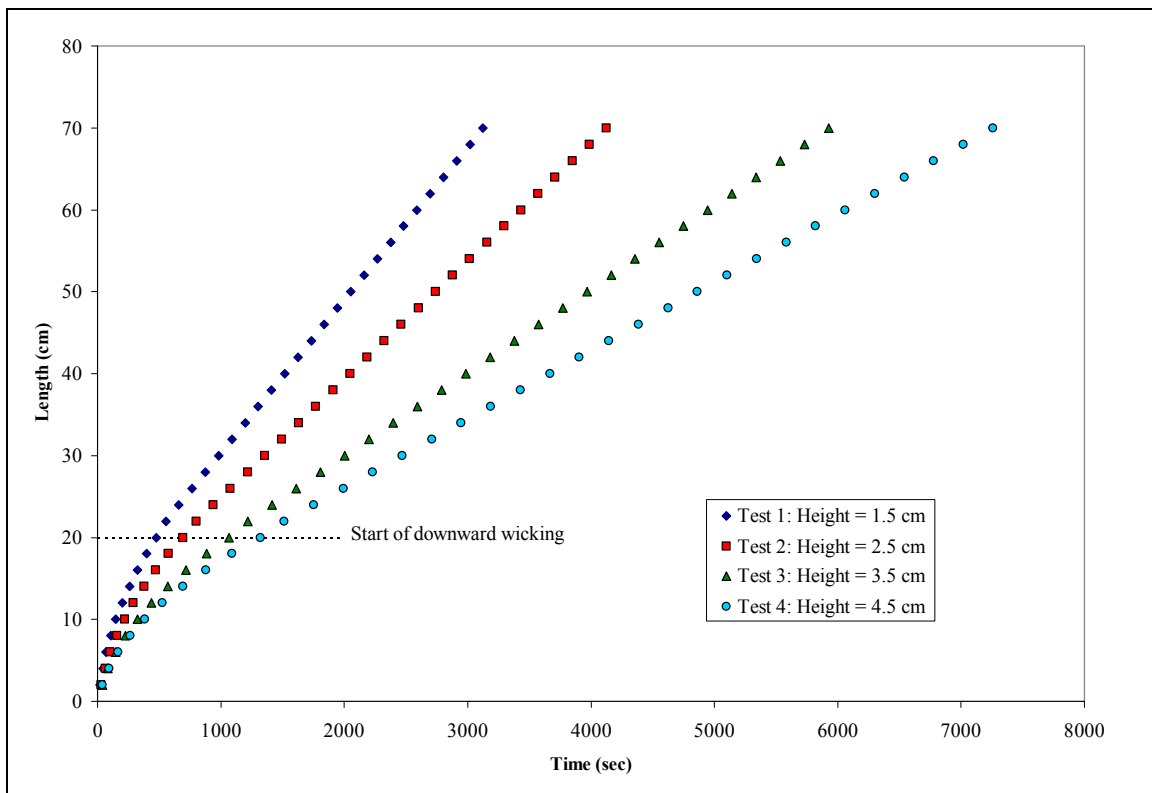


**Figure 4.9.1** – Horizontal-downward wicking test results for sample A.

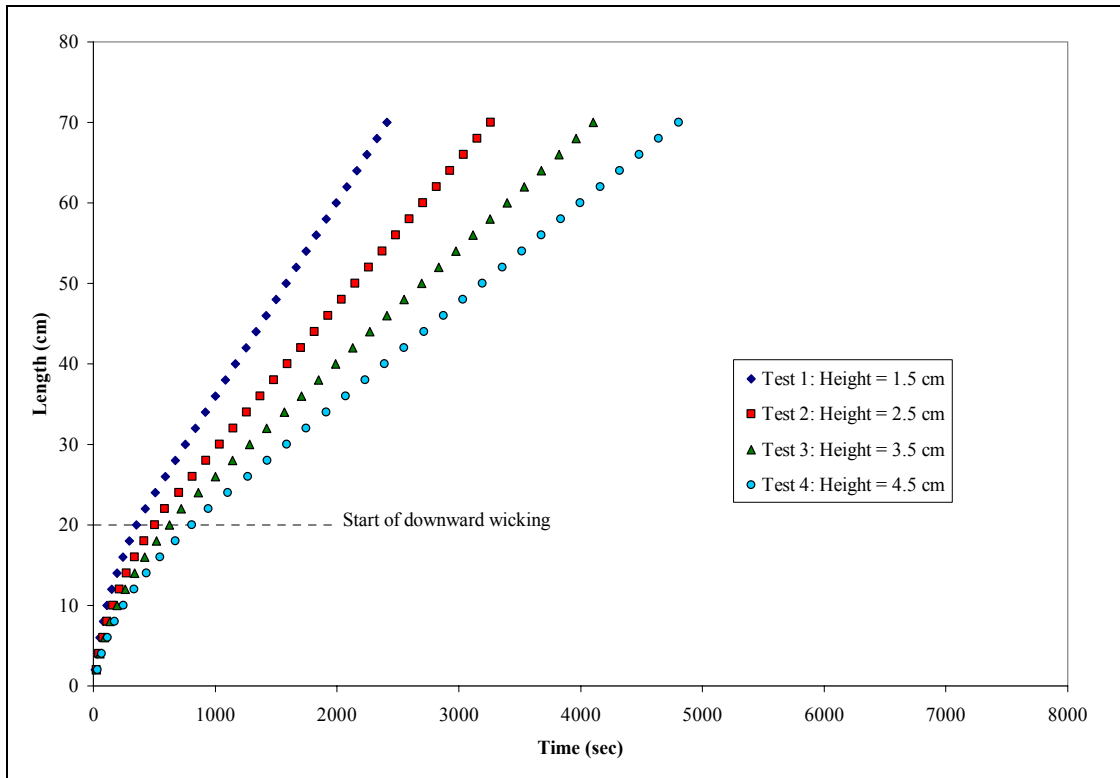


**Figure 4.9.2 – Horizontal-downward wicking test results for sample B**

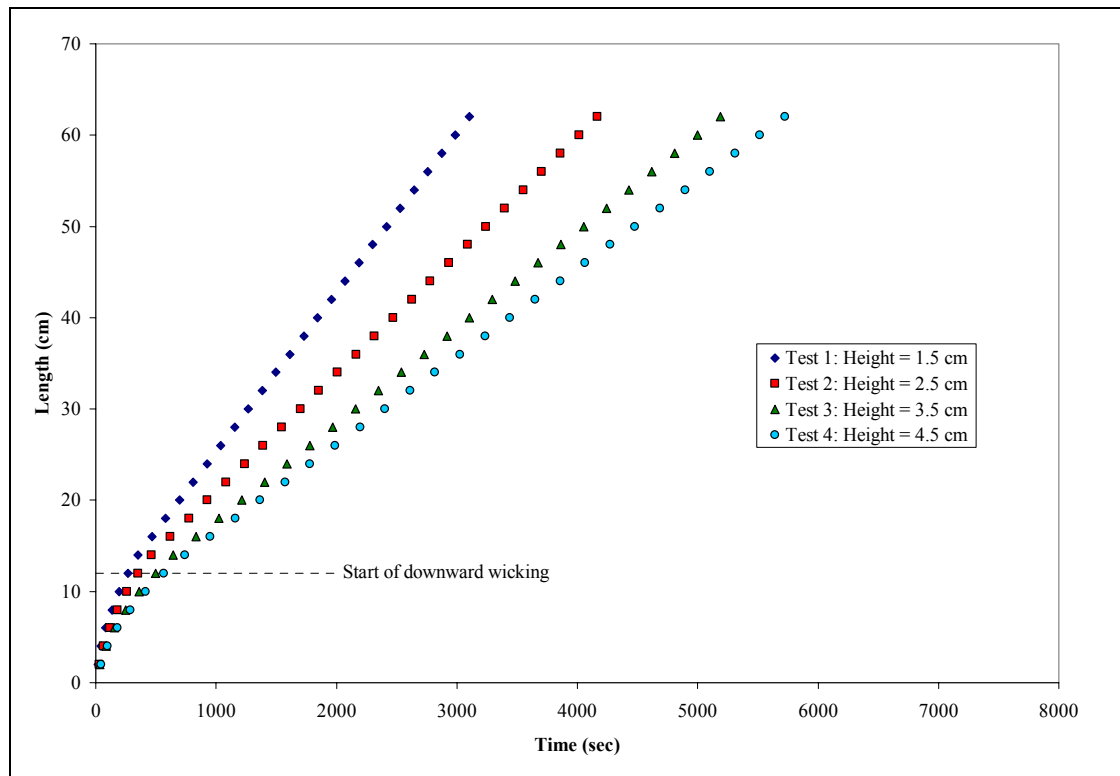


**Figure 4.9.3 – Horizontal-downward wicking test results for sample C.**

Graphical representation of the wicking tests clearly shows that sample B has a faster downward wicking flow rate over the other two samples. When comparing flow rates though, it must be noted that sample C was tested with a  $L_o$  of 12 centimeter. This decrease in horizontal length plays an important role when looking at flow rates alone. Remember as  $L_o$  increases, flow rate decreases due to viscous drag, therefore, it can not be concluded that sample C is a better wicking fabric than sample A based on these flow rates alone. To use the information collected from the horizontal-downward test method in order to better understand the individual wicking ability of each fabric, the horizontal and downward segments of the method need to be individually plotted and analyzed. Figures 4.9.4 through 4.9.6 represent the downward data obtained with the use of the method. The associated flow rates for each height are also recorded in these figures. These are the flow rates that will later be used to solve for permeability via Darcy's law.

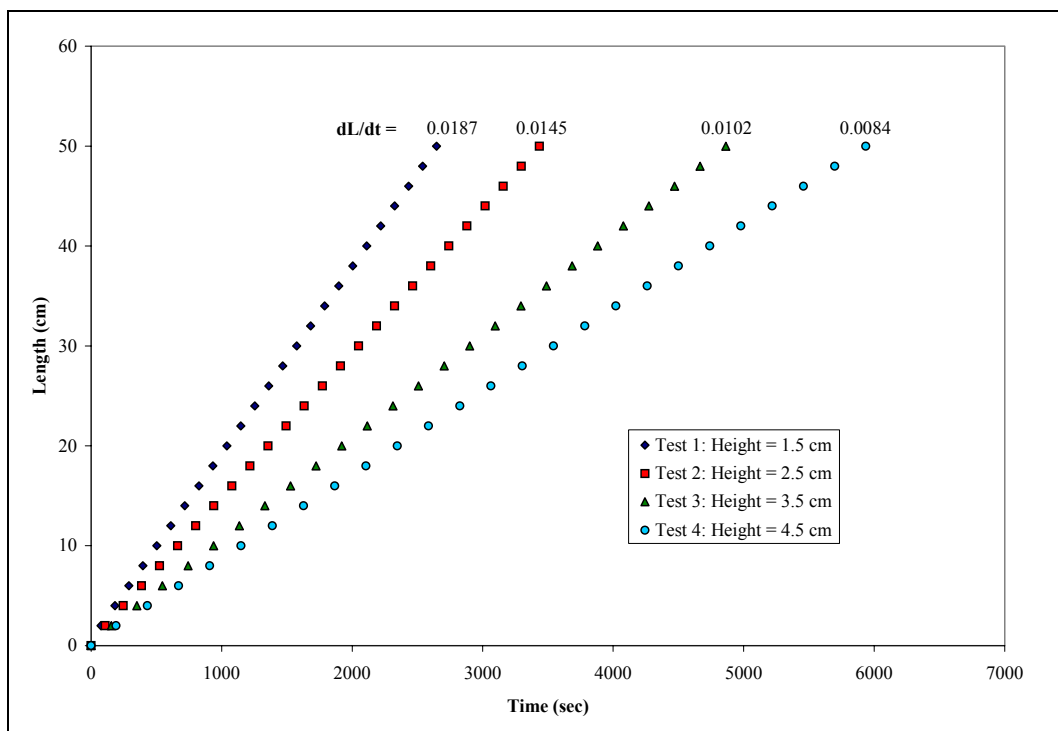


**Figure 4.9.4** – Downward data for sample A. Associated flow rates are labeled at the top of each set of data for a given test.  $L_o = 20$  cm.



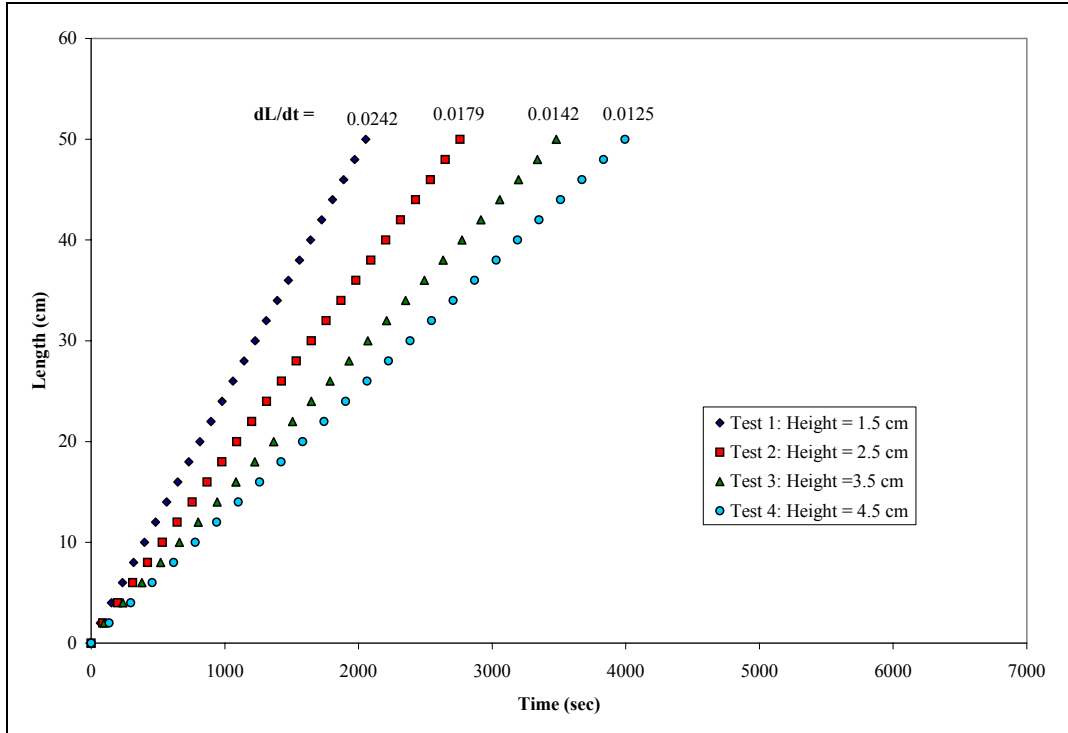


**Figure 4.9.5** – Downward data for sample B. Associated flow rates are labeled at the top of each set of data for a given test.  $L_o = 20$  cm.

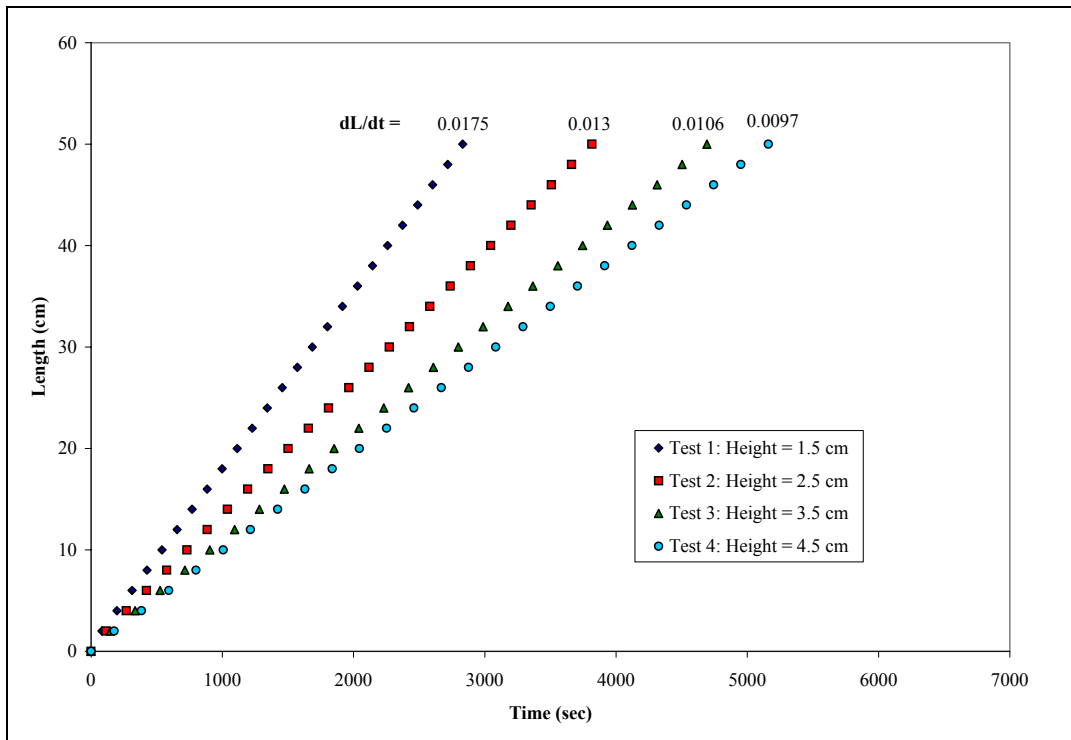


**Figure 4.9.6** – Downward data for sample C. Associated flow rates are labeled at the top of each set of data for a given test.  $L_o = 12$  cm.

It is interesting to see how sample C, even though it was tested at a much shorter horizontal length, still has the slowest downward wicking flow rate through the first two tests. For the third and fourth tests, though, it passes sample A. Again it is hard to just use this information. With the flow rates known, solving for permeability using Darcy's law has become one step closer. The fluid filling fractions (f) for each fabric at varying heights can be seen in Table 4.9.1. As stated before, the fluid filling fractions decrease as height is increased. This phenomenon is what was predicted earlier when discussing capillarity. It should be noted that these are the fluid filling fractions for both the horizontal and downward segments of the test method.

**Table 4.9.1** – List of fluid filling fractions at changing heights.

<b>Sample</b>	<b>Test 1</b>		<b>Test 2</b>		<b>Test 3</b>		<b>Test 4</b>	
	<b>Height (cm)</b>	<b>f</b>	<b>Height (cm)</b>	<b>f</b>	<b>Height (cm)</b>	<b>f</b>	<b>Height (cm)</b>	<b>f</b>
<b>A</b>	1.5	0.628	2.5	0.570	3.5	0.470	4.5	0.403
<b>B</b>	1.5	0.669	2.5	0.595	3.5	0.569	4.5	0.534
<b>C</b>	1.5	0.549	2.5	0.497	3.5	0.462	4.5	0.448

The data above clearly prove that as height increases, saturation level decreases. This was what was expected from the beginning. It can be seen how a small change in height affects a fabric's ability to take in moisture. It should be noticed how the change in height affected the float stitch fabric (A) more than the plain stitch fabrics (B and C). As mentioned in Section 4.6, this is due to the fact that the fabric has less yarn-yarn intersections. Will the construction of sample A affect its capillary pressure and permeability?

Using the horizontal section of the method, I was able to solve for the other needed variable, capillary pressure. As mentioned in Section 2.8, plotting horizontal wicking data as length versus the square root of time should give a straight line if the Lucas-Washburn equation

were to hold true. The slope of the line would be considered the wicking coefficient  $W_c$ . Once  $W_c$  is known, the effective capillary radius can be found using Equation 2.8.3. Remember, it is assumed that distilled water completely wets the fabrics, which would presumably give a contact angle of zero. The horizontal data for each sample is reported in Figures 4.9.7 thru 4.9.9.

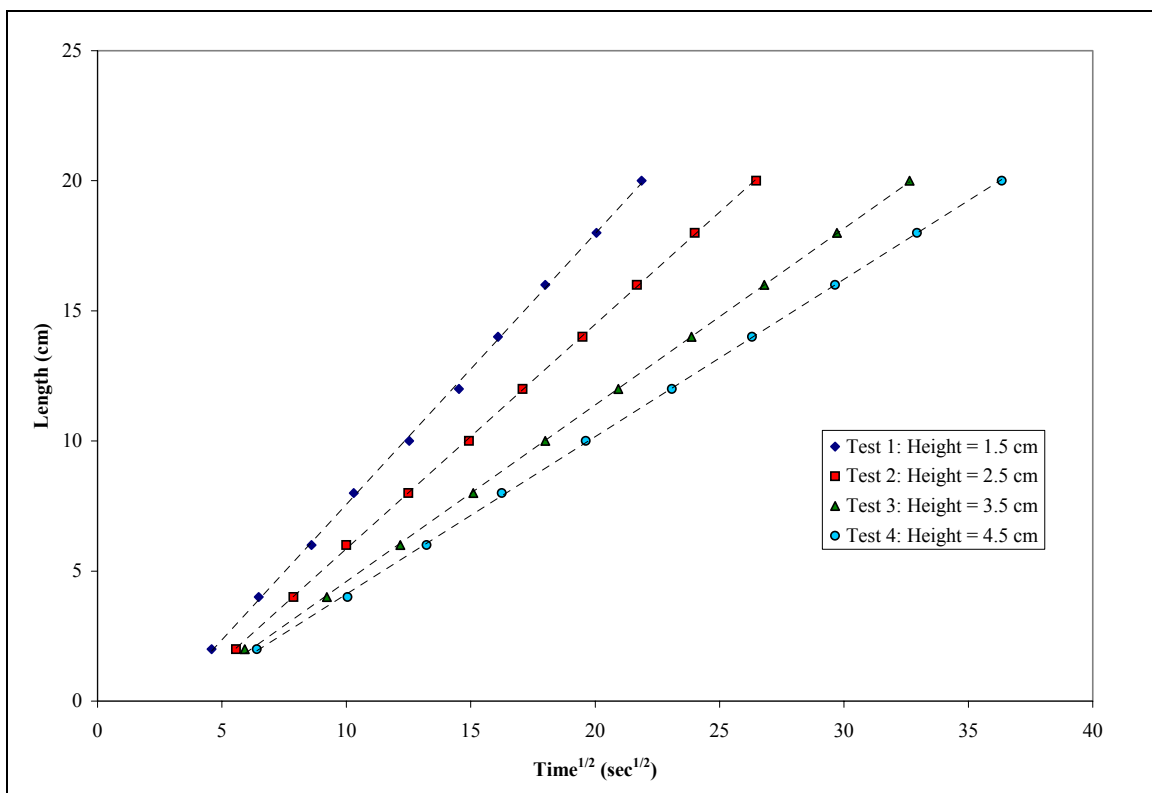


**Figure 4.9.7** – Horizontal segment of test method for sample A following the Lucas-Washburn equation.

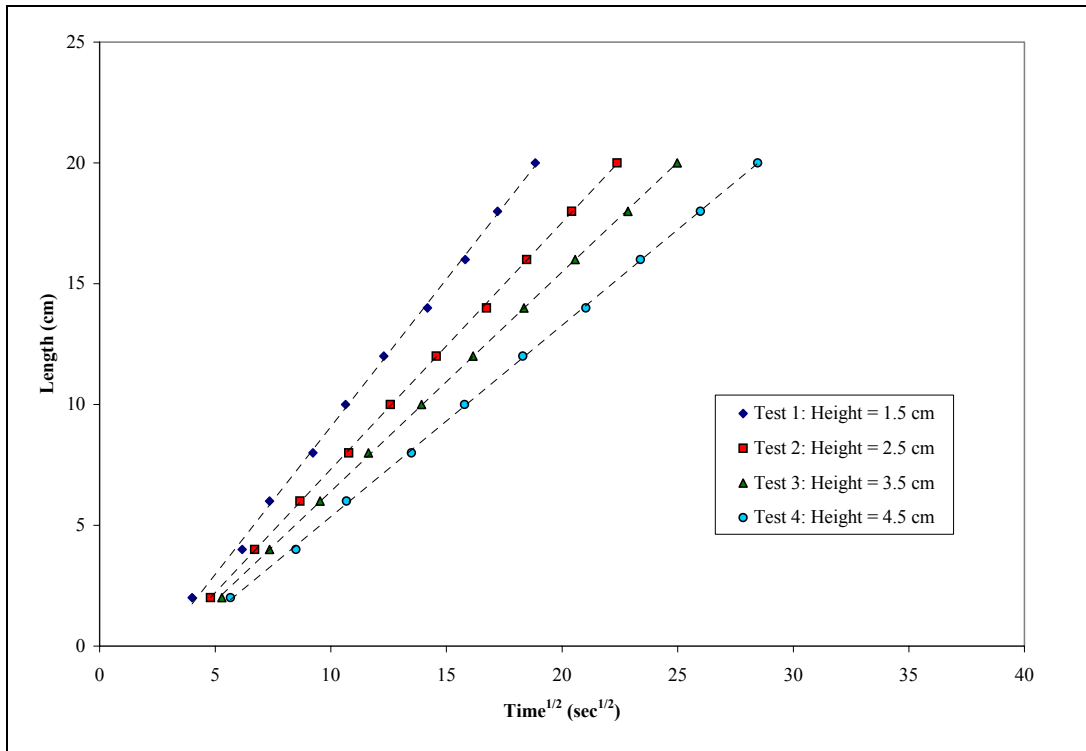


**Figure 4.9.8** – Horizontal segment of test method for sample B following Lucas-Washburn equation.

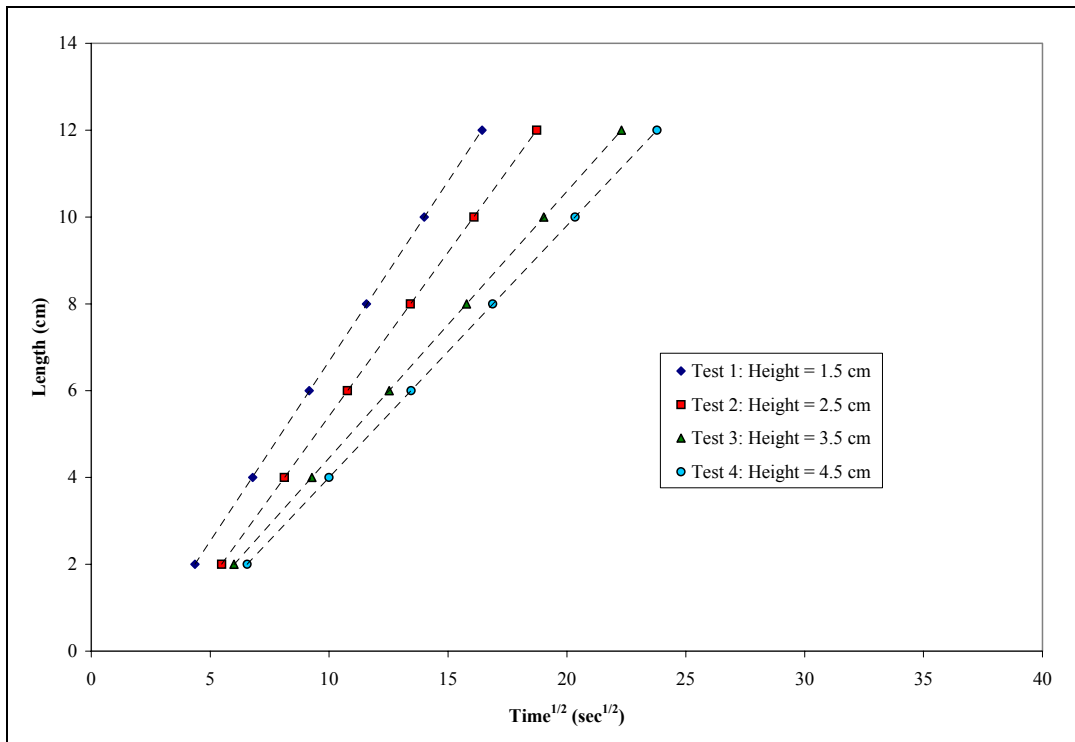


**Figure 4.9.9** – Horizontal segment of test method for sample C following Lucas-Washburn equation.

It is demonstrated by the best fit line of the data points above, that graphing length versus the square root of time for the horizontal segment of the test method does indeed give a straight line. It should be mentioned though, the Lucas-Washburn equation is used to define the flow through single capillaries and the graphs should pass through the origin. It can be seen that the lines do not pass through the origin. It has been reported in the literature<sup>28,30</sup> though, that single yarns tested using horizontal wicking produce a straight line that does pass through the origin. Unlike my proposed horizontal-downward wicking method, the method used to test the yarns did not have an initial vertical rise before horizontal wicking began, which may explain the non-zero y-intercept. Another theory has been proposed by Hollies *et al.*<sup>21</sup>, which describes the intercept as an “initiation period before the main capillary process could occur” and appears to be “related to the time required for the water to penetrate the surface of the yarns and fabrics.” This “wetting” time would change as the saturation level or fluid filling fraction changed. As saturation decreases, the wetting time should decrease because the amount of water to wet the fabric would decrease. In Table 4.9.2 below is a list of the wicking coefficients as well as the intercepts for each test height.

**Table 4.9.2** – List of wicking coefficients and y-intercepts for fabric samples.

Sample	Test 1 Height = 1.5 cm		Test 2 Height = 2.5 cm		Test 3 Height = 3.5 cm		Test 4 Height = 4.5 cm	
	$W_c$ (cm/s <sup>1/2</sup> )	y-int	$W_c$ (cm/s <sup>1/2</sup> )	y-int	$W_c$ (cm/s <sup>1/2</sup> )	y-int	$W_c$ (cm/s <sup>1/2</sup> )	y-int
<b>A</b>	1.041	-2.845	0.869	-2.763	0.678	-2.186	0.597	-1.938
<b>B</b>	1.214	-3.138	1.022	-2.891	0.907	-2.682	0.789	-2.569
<b>C</b>	0.829	-1.611	0.754	-2.125	0.614	-1.691	0.580	-1.804

Reviewing the data from Table 4.9.2, it is reported that the y-intercepts for each test do change. Assuming that the intercepts of such tests do not influence the validity of the Lucas-Washburn equation, one can use  $W_c$  and equation 2.8.3 to solve for the effective capillary radii in

the samples. Once the effective capillary radius for a given height is known, the capillary pressure can be solved using Equation 2.4.4. Table 4.9.3 below gives a complete list of the solved capillary radii  $R$  and capillary pressure  $P_c$  for each test and sample.

**Table 4.9.3** – Capillary radii and capillary pressure data for each sample at varying heights.

Sample	Test 1 Height = 1.5 cm		Test 2 Height = 2.5 cm		Test 3 Height = 3.5 cm		Test 4 Height = 4.5 cm	
	R ( $\mu\text{m}$ )	$P_c$ (dynes/cm <sup>2</sup> )	R ( $\mu\text{m}$ )	$P_c$ (dynes/cm <sup>2</sup> )	R ( $\mu\text{m}$ )	$P_c$ (dynes/cm <sup>2</sup> )	R ( $\mu\text{m}$ )	$P_c$ (dynes/cm <sup>2</sup> )
<b>A</b>	2.97	$4.89 \times 10^5$	2.07	$7.02 \times 10^5$	1.26	$1.15 \times 10^6$	0.98	$1.48 \times 10^6$
<b>B</b>	4.05	$3.60 \times 10^5$	2.87	$5.04 \times 10^5$	2.49	$5.85 \times 10^5$	1.71	$8.55 \times 10^5$
<b>C</b>	1.89	$7.71 \times 10^5$	1.56	$9.32 \times 10^5$	1.04	$1.40 \times 10^6$	0.92	$1.57 \times 10^6$

As predicted by vertical wicking, sample C does have the smallest pore sizes and exhibits the greatest capillary pressure. Contrary to what was predicted by vertical wicking, sample A does not contain the largest pore sizes. Sample A, based on effective capillary radius, should have been able to transport liquid to a greater height when compared to Sample B, but due to its float stitch construction, it could not. The lack of yarn intersections, and therefore lack of new reservoirs, causes moisture in sample A to stop at a lower height than one would expect based on the data in Table 4.8.3 and the laws that govern capillary flow. This again proves how erroneous a vertical wicking test can be.

The data in Table 4.9.3 also proves that capillary pressure is not a constant, but changes as the height increases. Just as predicted, the capillary pressure increases as effective pore size and fluid filling fraction decreases. This makes sense, because a smaller capillary would take a greater amount of pressure to move moisture through it than a larger one would. Using this information one could acquire an intrayarn pore size distribution based on saturation levels. Now that capillary pressure is known, one can use this pressure and the flow rates found from

downward wicking to properly solve Darcy's law for permeability at varying saturation levels. Permeability was found using equation 2.7.2 and is displayed in Table 4.9.4 below.

**Table 4.9.4** – Solved permeability for fabric samples using Darcy's law. The units are in  $\text{cm}^2$

<b>Sample</b>	<b>Test 1</b> Height = 1.5 cm	<b>Test 2</b> Height = 2.5 cm	<b>Test 3</b> Height = 3.5 cm	<b>Test 4</b> Height = 4.5 cm
<b>A</b>	$7.656 \times 10^{-9}$	$4.140 \times 10^{-9}$	$1.774 \times 10^{-9}$	$1.134 \times 10^{-9}$
<b>B</b>	$1.349 \times 10^{-8}$	$7.076 \times 10^{-9}$	$4.875 \times 10^{-9}$	$2.944 \times 10^{-9}$
<b>C</b>	$2.727 \times 10^{-9}$	$1.676 \times 10^{-9}$	$9.064 \times 10^{-10}$	$7.405 \times 10^{-10}$

The data show that sample B has the greatest permeability for every height. If in fact permeability and capillary pressure are indeed the fundamental properties of wicking, then sample B would be the best wicking fabric tested. It had the highest fluid filling fractions, fastest flow rates, and highest permeabilities for each test.

The data in Table 4.9.4 also confirms how the level of saturation within a fabric affects its permeability. As predicted, when saturation decreases, permeability decreases. In Figure 4.9.10, permeability is graphed as a function of fluid filling fraction (saturation) for samples A, B, and C.

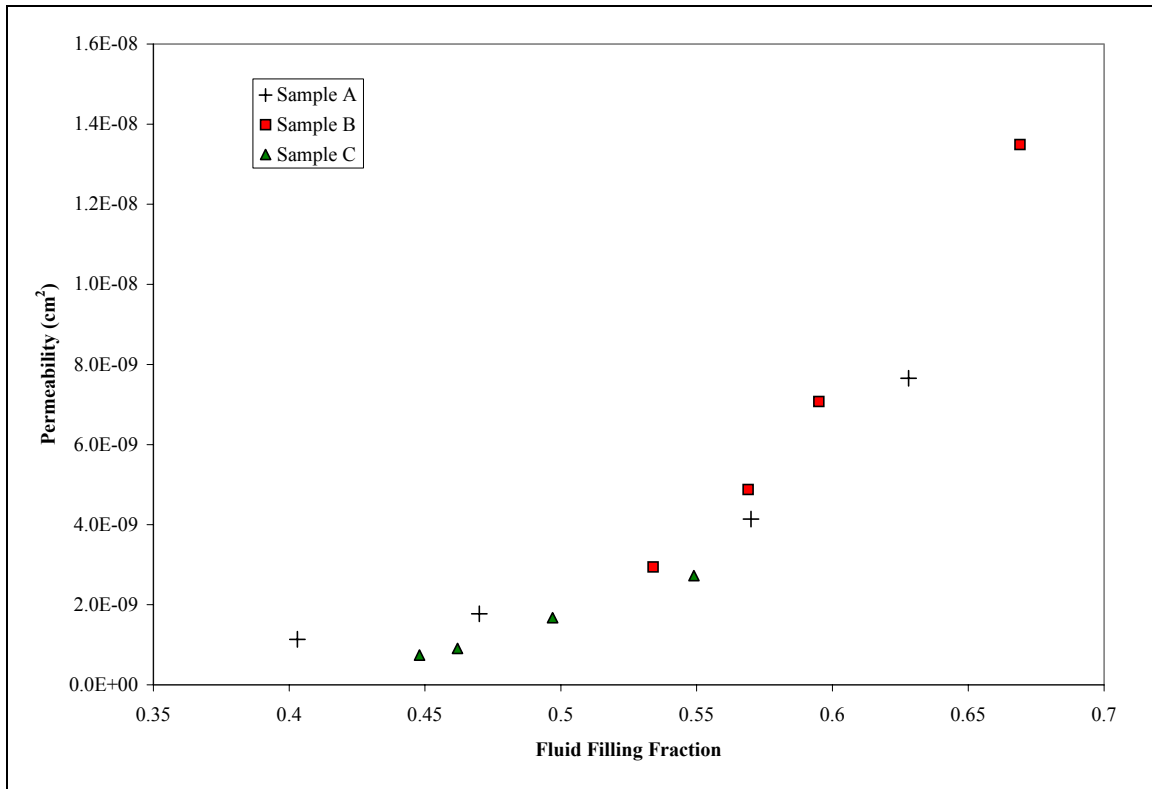


**Figure 4.9.10** – Plot of permeability as a function of fluid filling fraction. Sample B has the highest permeability at higher saturation, but drops below that of sample A after a fluid filling fraction of 0.55.

It can be observed that under a fluid filling fraction of around 0.55 the permeability of sample B drops below that of sample A. It demonstrates how saturation within a fabric affects its permeability, and therefore its ability to wick moisture. This indicates that sample B, containing large capillaries, would not sustain fluid flow as well as sample A at lower saturation levels. This phenomenon is due to the differences in pore size within the samples. Sample A's smaller pores are easily filled at lower saturation levels, contrary to the larger pores of sample B, which do not fill. This allows sample A to have a higher permeability at lower saturation than sample B.

Overall, the fabric that was constructed with yarns containing the largest sized capillaries was the best wicking material above a saturation level of 0.55. With its comparatively fast flow rates and high permeabilities, sample B outperformed the other two test samples in this range of



saturation levels. Once the saturation of the fabric samples dropped below 0.55, sample A, with its relatively small effective capillary radii, was the best wicking material. This helps conclude that a company could not deem their product the best wicking material in a generic definition; all conditions must be known. If someone sweats profusely, then a fabric with large capillary radii would wick the perspiration the best, but if one does not sweat very much then a fabric with smaller capillary radii would be preferred. Perhaps, a fabric made with intermeshed thick and thin yarns could combine the properties of both fabrics. This intermeshed construction would also provide a fabric with a broad pore size distribution, and thus a wide range of permeabilities at varying saturation levels. This testing shows how important fabric structure is for wicking moisture. All the samples were made of polyester, yet performed very differently. It would be interesting to see how similar constructed fabrics made of natural fibers would perform compared to these made of synthetic fibers.

## **Chapter 5**

### **Conclusions**

- Capillary pressure and permeability are not constants, but are functions of the level of saturation within the fabric.
- Changing vertical rise of horizontal-downward test allows solving for capillary pressure and permeability at varying saturation levels.
- Fabric with yarns containing the larger effective capillary radii had higher permeabilities at high levels of saturation.
- Once saturation dropped below a certain level, the yarns with smaller effective capillary radii were able to sustain higher permeabilities.
- One can not define wicking at only one condition – a range of conditions must be tested in order to fully understand the ability of a fabric to wick moisture.

## **Chapter 6**

### **Recommendations**

All the fabrics tested in this study were made polyester. It was seen that the structure and construction of the fabric made a noticeable difference in wicking. It is my recommendation to test similar constructed fabrics made of different types of fibers. The fibers should be made of natural and synthetic sources. This type of study would better put to rest the arguments made about fiber type. Would fiber type make a difference or is it only construction that plays a role in wicking. The testing of the rougher natural fibers may also require the need to test the theory about contact angle. The assumption made about a zero contact angle may not hold true for every fiber type and should be considered.

The heights chosen only tested the fabrics at a small array of saturations. It is my recommendation to conduct the tests at greater height intervals in order to acquire permeability and capillary pressure data over a wider range of saturation levels. Also, it was shown at the end of the report how a plain stitch fabric compared to a thinner float stitch fabric. The fabrics tested should be similar in yarn size and thickness, but different in construction type. Many types of knits should be tested to classify the best wicking pattern.

It should also be noted that yarn twist was not known for these samples. Twist may have also be a deciding factor for how a fabric wicks moisture. It would make sense that a yarn with high twist would wick moisture slower than a yarn with low twist. Yet the low twist yarn would sustain flow even at lower saturation levels, due to the reduced size of the pores. Testing fabrics with known yarn twist would be beneficial for the study of wicking.

## References

- (1) Zhang, P., Gong, R. H., Yanai, Y., and Tokura, H., Effects of Clothing Material on Thermoregulatory Responses, *Textile Research Journal*. **2002**, 72, 83-89.
- (2) Watt, I. C., Moisture Interaction: A Vital Factor in Performance, Comfort, and Appearance.
- (3) Sweeney, M., and Branson, D., Sensorial Comfort, *Textile Research Journal*. **1990**, 60, 371-377.
- (4) Rossi, R. In *International Man-Made Fibres Congress*: Dornbirn, Austria, 2000.
- (5) Weber, M., Frei, G., Bruhwiler, P. A., Herzig, U., Huber, R., and Lehmann, E., Neutron Radiography Measurement of the Moisture Distribution in Multilayer Clothing Systems.
- (6) Crow, R. M., The Interaction of Water with Fabrics, *Textile Research Journal*. **1998**, 68, 280-288.
- (7) Tortora, P. G., Collier, B. J., "Understanding Textiles," 5 ed., Prentice-Hall, Inc., Upper Saddle River, NJ, 1997.
- (8) Harnett, P. R., and Mehta, P. N., A Survey and Comparison of Laboratory Test Methods for Measuring Wicking, *Textile Research Journal*. **1984**, 54, 471-478.
- (9) Hsieh, Y.-L., Liquid Transport in Fabric Structures, *Textile Research Journal*. **1995**, 65, 299-307.
- (10) Marchal, J.-M., Modeling Capillary Flow in Complex Geometries, *Textile Research Journal*. **2001**, 71, 813-821.
- (11) <http://www.polartec.com/contentmgr/showdetails.php/id/209#tech>.
- (12) Ghali, K., Jones, B., and Tracy, J., Experimental Techniques for Measuring Parameters Describing Wetting and Wicking in Fabrics, *Textile Research Journal*. **1994**, 64, 106-111.
- (13) Kissa, E., Wetting and Wicking, *Textile Research Journal*. **1996**, 66, 660-668.
- (14) Schwartz, A. M., Capillarity: Theory and Practice.
- (15) Miller, B., Critical Evaluation of Upward Wicking Tests, *International Nonwovens Journal*. **2000**, 9, 35-40.
- (16) Minor, F. M., and Schwartz, A. M., Pathways of Capillary Migration of Liquids in Textile Assemblies, *American Dyestuff Reporter*. **1960**, 49, 37-42.
- (17) <http://www.myerscarpet.com/>.
- (18) Dullien, F. A. L., "Porous Media: Fluid Transport and Pore Structure," 2 ed., Academic Press, London, 1992.
- (19) Greenkorn, R. A., "Flow Phenomena in Porous Media," Marcel Dekker, Inc., New York, 1983; Vol. 16.
- (20) Adams, K. L., and Rebenfeld, L., In-Plane Flow of Fluids in Fabrics: Structure/Flow Characterization, *Textile Research Journal*. **1987**, 57, 647-654.
- (21) Hollies, N. R. S., Kaessinger, M. M., Watson, B. S., and Bogaty, H., Water Transport Mechanisms in Textiles Materials Part II: Capillary-Type Penetration in Yarns and Fabrics, *Textile Research Journal*. **1957**, 8-13.
- (22) Hollies, N. R. S., Kaessinger, M. M., and Bogaty, H., Water Transport Mechanisms in Textile Materials Part I: The Role of Yarn Roughness in Capillary-Type Penetration, *Textile Research Journal*. **1956**, 26, 829-835.

- (23) <http://fabriclink.com/pk/coolmax/home.html>.
- (24) McLaughlin, J. R., Trounson, M. E., Stewart, R. G., and McKinnon, A. J., *Textile Research Journal*. **1988**, 58, 501.
- (25) Saville, B. P., "Physical Testing of Textiles," Woodhead Publishing Limited, Cambridge, England, 2000.
- (26) Warner, S. B., "Fiber Science," Prentice-Hall, Inc., Englewood Cliffs, NJ, 1995.
- (27) Chen, X., Kornev, K. G., Kamath, Y. K., and Neimark, A. V., The Wicking Kinetics of Liquid Droplets into Yarns, *Textile Research Journal*. **2001**, 71, 862-869.
- (28) Kamath, Y. K., Hornby, S. B., Weigmann, H. D., and Wilde, M. F., Wicking of Spin Finishes and Related Liquids into Continuous Filament Yarns, *Textile Research Journal*. **1994**, 64, 33-40.
- (29) Katch, "Exercise Physiology-Energy, Nutrition and Human Performance," 4 ed., Williams & Wilkins, 1996.
- (30) Perwuelz, A., Mondon, P., and Caze, C., Experimental Study of Capillary Flow in Yarns, *Textile Research Journal*. **2000**, 70, 333-339.